UNIVERSIDAD COMPLUTENSE DE MADRID
FACULTAD DE MEDICINA

TESIS DOCTORAL

Human CD247 deficiency (Deficiencia humana de CD247)

MEMORIA PARA OPTAR AL GRADO DE DOCTOR

PRESENTADA POR

Ana Victoria Marin Marin

Directores

José Ramón Regueiro González-Barros
George Tsokos

Madrid

UNIVERSIDAD COMPLUTENSE DE MADRID

FACULTAD DE MEDICINA

TESIS DOCTORAL

Human CD247 Deficiency (Deficiencia humana de CD247)

MEMORIA PARA OPTAR AL GRADO DE DOCTOR

PRESENTADA POR

Ana Victoria Marin Marin

DIRECTOR

José Ramón Regueiro González-Barros
George Tsokos

Departamento de Inmunología,
Oftalmología y ORL (IOO)
Universidad Complutense de Madrid

Human CD247 deficiency (Deficiencia humana de CD247)

Candidata Doctorado Bioquímica, Biología Molecular y Biomedicina:

Ana Victoria Marín Marín

Director:

José R**amón** Regueiro González Barros

Co-director:

George Tsokos

Madrid, 2020

ACKNOWLEDGEMENTS

Gracias:

A mi director de tesis, José R. Regueiro, por permitirme aprender y disfrutar de la ciencia y la academia. Ha sido una larga etapa de aprendizaje donde hemos pasado momentos estresantes, pero otros muy intrigantes y divertidos que siempre recordaré y relataré.

A mi codirector de tesis, George C. Tsokos, por brindarme la oportunidad de conocer otro país y un sistema de trabajo muy diferente y enriquecedor. A mis compañeros de Boston que tanto me enseñaron y motivaron.

A mi tutor Javier Fernández Ruiz por ayudarme tan amablemente en los procesos tediosos del doctorado.

A los pacientes y médicos que han facilitado la realización de todos los experimentos de este trabajo.

A los miembros del consejo de sabios del departamento, pues siempre han estado disponibles para resolver dudas y aportar ideas, además de las celebraciones con el cali mágico. A los profesores del departamento por la ayuda siempre brindada.

A mis compañeros de bancada históricos (Inmunitos, sí ya era hora de defender la tesis) y presentes; inmunólogos, complementólogos y amigas, conservo muy buenos recuerdos de todas las temporadas y las que aun nos quedan.

A mis amigas Immune-Ladies, os debo una barbacoa y un abrazo.

A mi familia, por el apoyo de todo tipo durante estos largos años y buenos momentos entre uvas y almendras.

Y finalmente a mis perros, por tantas horas de espera culminadas con lametones infinitos.

TABLE OF CONTENTS

SUMMARY

The T-cell receptor (TCR) is the antigen receptor of T lymphocytes. In humans it is composed of one variable heterodimer (TCRαβ or γδ), two invariant heterodimers (CD3εγ and CD3εδ) and one invariant homodimer (CD247, also called ζζ). It has a crucial role during T-cell selection and activation, so that mutations in the genes codifying for TCR chains cause immunodeficiency disease (TCRID) of varying severity depending on the affected protein. TCRID cases are extremely rare but valuable models to understand human TCR biology, considering that mouse models or human genetically modified tumoral cell lines do not fully recapitulate the behaviour of the human TCR.

Our objectives were a) to characterize the T-cell phenotype of a new CD247-deficient patient and establish the pathognomonic features of the disease, and b) to study how homozygous or heterozygous mutations in *CD247* affected the assembly and trafficking of the TCR from the endoplasmic reticulum (ER) to the T-cell surface as well as its recycling and degradation.

To that end, we studied a) blood T lymphocytes from the patient and other family members and b) T-cell lines derived from them, using the following techniques: flow cytometry, Western blot, immunoprecipitation, confocal microscopy and T-cell culture and functional assays.

The results in primary T cells indicated that the new reported *CD247* mutation (c.2T>C) codified for a truncated protein that was undetectable and caused a severe surface TCR expression and signaling defect. However, a small percentage of T cells recovered TCR expression and signaling levels of carriers due to two different somatic mutations, a second site and a revertant mutation. We devised a fast and simple intracellular flow cytometry protocol to diagnose TCRID in blood.

The T-cell lines nicely recapitulated the phenotype of partial (+/—) or complete (—/—) CD247-deficient primary αβ T cells. The immunoprecipitation assays showed that CD3 εγ and εδ heterodimers were bound to TCRαβ in +/+ and +/— cells, but only to TCRα in —/— cells, weakening the existence of a hexameric αβεγεδ TCR before CD247 assembly. Engaged surface TCR of CD247-negative TCR ensembles were internalized but not recycled, supporting a central role of CD247 in TCR recycling, but not internalization. The confocal microscopy studies indicated that CD3 chains accumulated in the ER rather than in the Golgi apparatus in —/— cells, suggesting that CD247 is incorporated to the TCR in the ER in normal T cells, as confirmed in +/+ and +/— cells. Inhibition experiments indicated that surface TCR increased in both CD247-deficient and –sufficient T cells when the proteasome, but not the lysosome, was blocked, supporting a proteasome- rather than lysosome-dependent TCR degradation pathway.

In conclusion, mild lymphopenia and functional revertant somatic mosaicism should not confound the fact that CD247 deficiency is a very severe condition that requires urgent transplantation, but easy to diagnose by intracellular flow cytometry or by the surface TCR phenotype of obligate carriers. CD247-deficient T-cell lines recapitulated primary T cells and informed human TCR assembly and degradation dynamics.

RESUMEN

El *T-cell receptor* (TCR) es el receptor de antígenos de los linfocitos T. En humanos está compuesto por un heterodímero de cadenas variables (αβ or γδ), dos heterodímeros invariantes (CD3εγ y CD3εδ) y un homodímero invariante (CD247, también llamado ζζ). El TCR desempeña un papel esencial en los linfocitos T durante su selección tímica y activación, por lo que mutaciones en los genes que codifican las cadenas del TCR se asocian a un tipo de inmunodeficiencia (IDTCR), que varía en gravedad dependiendo de la cadena afectada. Los casos de IDTCR son extremadamente raros pero son valiosos modelos para comprender la biología del TCR humano, ya que los modelos múridos o líneas tumorales humanas genéticamente modificadas no lo recapitulan fielmente.

Nuestros objetivos fueron a) caracterizar el fenotipo de los linfocitos T en un nuevo caso de deficiencia de CD247 y establecer las características patognomónicas de la enfermedad, y b) estudiar cómo las mutaciones en homocigosis o heterocigosis en *CD247* pueden afectar al ensamblaje y tráfico del TCR desde el retículo endoplásmico (RE) hasta la superficie celular, así como su reciclaje y degradación.

Para ello, estudiamos a) linfocitos T aislados de muestras de sangre venosa del paciente y su familia y b) líneas celulares de linfocitos T derivadas de éstos, utilizando las siguientes técnicas: citometría de flujo, Western blot, inmunoprecipitación, microscopía confocal, cultivos in vitro de linfocitos T y ensayos funcionales.

Los resultados en linfocitos T primarios indicaron que la nueva mutación en *CD247* (c.2T>C) codificaba para una proteína truncada que resultó indetectable y provocaba una dramática disminución en los niveles de superficie y de señalización del TCR. Sin embargo, un pequeño porcentaje de células T recuperaba el nivel de expresión y señalización del TCR de los portadores debido a dos mutaciones somáticas, una mutación en un sitio del genoma adicional y una en el original. Establecimos un procedimiento rápido y sencillo de citometría intracelular para diagnosticar IDTCR en muestras de sangre venosa.

Las líneas de linfocitos T generadas recapitulaban el fenotipo de la deficiencia parcial (+/—) o completa (—/—) de CD247 en linfocitos αβ primarios.

Los experimentos de inmunoprecipitación demostraron que los heterodímeros CD3εγ y εδ se unían al TCRαβ en las células +/+ y +/—, pero sólo a TCRα en las —/—, debilitando la existencia propuesta de un TCR hexamérico αβεγεδ antes de su unión a CD247. Como era de esperar, el TCR sin CD247 sí señalizaba para su internalización pero sin embargo, no podía reciclarse, lo que apoya un papel central de CD247 en el reciclaje del TCR, pero no en su internalización. Los resultados de microscopía confocal demostraron que cuando CD247 estaba ausente, las cadenas CD3 se acumulaban en el RE y no en el Golgi, indicando que CD247 se incorpora al TCR en el RE en linfocitos T normales, lo que se confirmó en células +/+ y +/—. Los ensayos de inhibición demostraron que los niveles de TCR en membrana aumentaron en las líneas CD247-deficientes y -suficientes tras bloquear el proteasoma, pero no el lisosoma, lo cual apoya la primera ruta de degradación del TCR frente a la segunda.

En conclusión, la existencia de linfopenia leve y mosaicismo somático funcional no deben distraernos de que la deficiencia de CD247 es una patología muy grave que requiere trasplante urgente de progenitores hematopoyéticos, pero que es fácil de diagnosticar mediante citometría intracelular o por el fenotipo TCR de membrana en portadores obligados. Las líneas celulares de linfocitos T deficientes de CD247 recapitulan el fenotipo de los linfocitos T primarios y ayudan a entender la dinámica de ensamblaje y degradación del TCR humano.

ABBREVIATIONS

BFA	Brefeldin A
CFSE	Carboxyfluorescein diacetate succinimidyl ester
CHL	Chloroquine
CID	Combined immunodeficiency
CMV	Cytomegalovirus
DN	Double negative
DP	Double positive
ER	Endoplasmic reticulum
ETP	Early thymic progenitor
E. lys	Enriched whole-cell lysate
Geo-MFI	Geometric mean fluorescence intensity
IL-2	Interleukin-2
IP	Immunoprecipitation
ITAM	Immunoreceptor tyrosine-based activation motifs
HD	Healthy donor
HSC	Hematopoietic stem cell
HSCT	Haploidentical stem cell transplantation
HVS	Herpesvirus Saimiri
HTLV-1	Human T-lymphotropic virus type 1
MFI	Mean fluorescence intensity
PBMC	Peripheral blood mononuclear cells
PHA	Phytohemagglutinin
TCR	T-cell receptor
TCRID	TCR-immunodeficiency disease or *inmunodeficiencia del TCR*
SCID	Severe combined immunodeficiency
SEM	Standard error of the mean
pZAP70	Phospho-zeta-associated protein
pERK	Phospho-extracellular signal–regulated kinase
vs	Versus

1. INTRODUCTION

1.1. TCR/CD3/CD247 complex

T lymphocytes detect the presence of antigens by means of a cell surface multi-protein complex termed the T-cell receptor (TCR). In humans, the TCR is composed of a variable heterodimer (either TCRαβ or TCRγδ), two invariant heterodimers (CD3γε and CD3δε), and an invariant homodimer (CD247 or ζζ) (Call *et al.*, 2002; Dong *et al.*, 2019). The variable proteins are involved in antigen recognition, while the invariant proteins participate in assembly and surface expression of the TCR complex, and in the delivery of intracellular signals through the phosphorylation of tyrosine residues within the immunoreceptor tyrosine-based activation motifs (ITAM) of their cytoplasmic tails (Love *et al.*, 2010; Malissen *et al.*, 1999).

1.2. TCR dynamics

From the synthesis of TCR chains to their expression on the cell surface as a octameric complex, the TCR subunits undergo a finely regulated process of assembly and secretion via the endoplasmic reticulum (ER) and the Golgi apparatus. The total amount of surface TCR expression and function will depend on the synthesis of each TCR chain, the success of the assembly of the heterodimers or homodimer and the octameric complex itself, the location of the structures that sequentially have been able to be formed at the plasma membrane and within intracellular vesicular compartments, the ability of the TCR to transduce signals and the degradation of each subunit and of the partial or complete TCR (Alcover *et al.*, 2018).

About the required steps to the correct trafficking and assembly of each piece of the TCR, the bibliography indicates that the TCR chains interact between them by ionic and covalent bonds located in the transmembrane regions, first formed the CD3εδ/ and CD3εγ heterodimers, then they bind preferentially to TCRα and TCRβ, respectively, and then CD247 homodimer is joined to the complex (Fig Intro 1) (Borroto *et al.*, 1998; Call *et al.*, 2005; Malissen *et al.*, 1999; Natarajan *et al.*, 2016). The formation of the heterodimers and the hexameric complex is supposed to take place in the ER but the incorporation of the CD247 dimer was described to be in Golgi compartment (Call *et al.*, 2004; Dietrich *et al.*, 1999), according mouse or Jurkat cell lines data. The data in these cell lines indicated that whenever the hexameric TCR was not able to be assembled, the TCRα was retained in the Golgi meanwhile the CD3 chains were located still in ER, suggesting that the final step of TCR assembly may take place in the Golgi apparatus (Dietrich *et al.*, 1999). When these authors tested the TCR trafficking in absence of CD247 by using the mouse CD247-deficient MA5.8 cell line, they observed that the CD3 chains were retained in the Golgi. As quality control mechanism, CD3ε, CD3γ and TCRα present ER retention signals that ensure the exportation of a correctly assembled structure to the cell surface (Bonifacino *et al.*, 1991; Carrasco *et al.*, 2001; Delgado *et al.*, 2005; Mallabiabarrena *et al.*, 1992), what give at least one functional ER retention signal for each intermediate that makes sure that a full signaling-competent TCR complex is expressed on the cell surface.

An important mechanism that regulates the capacity of a T-cell to respond to TCR signaling is the regulation of the amount of the complex on the cell surface (Compeer *et al.*, 2018). In resting conditions, the TCR is immersed in an endocytosis and re-expression cycle between cell surface and recycling compartment that relies on clathrin-dependent or independent endocytosis and other pro-

teins (Alcover *et al.*, 2018; Dietrich *et al.*, 1994; Martinez-Martin *et al.*, 2011; Monjas *et al.*, 2004), hereafter referred as TCR-recycling cycle. The downmodulation of bystander TCR requires protein kinase C, protein-tyrosine kinase activity and the dileucine endocytosis motif of CD3γ (Dietrich *et al.*, 1994; Monjas *et al.*, 2004). So, the maintaining or certain amount on the cell surface and also a backup on the recycling compartment is important to develop the proper TCR signaling and to be ready for the next. In regular conditions, an assay to address how is the functioning of the TCR-recycling cycle is the incubation of the T-cells in presence of brefeldin A (BFA), a reversible anterograde protein trafficking inhibitor drug, so after certain time it can be observed a decrease of the TCR on the cell surface that should be restored if the cycle is working properly and new synthetize TCR complex travels to the cell surface (Liu *et al.*, 2000). In case of the engagement of the TCR it is also internalized, and some can be recycled the cell surface but certain amount of it is derived to degradation (Liu *et al.*, 2000).

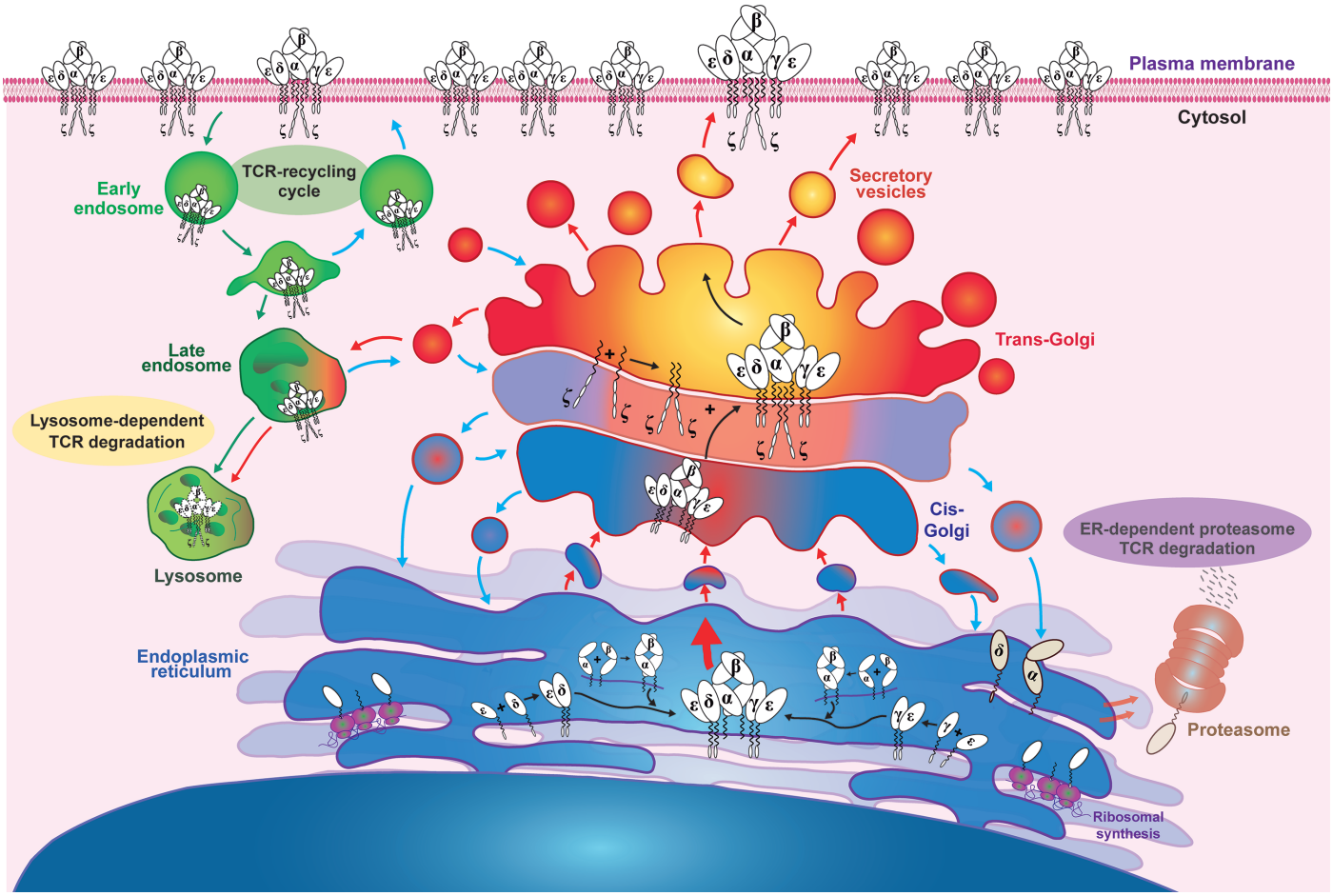

Figure Intro 1. TCR synthesis, assembly and trafficking from the endoplasmic reticulum (ER) to the plasma membrane. TCR-recycling cycle is represented through early endosome compartment. Lysosome- and proteasome-dependent TCR degradation mechanism are considered. ζ refers to CD247, both names can be used equally. The information of the figure has been collected from the literature indicated in the manuscript.

As indicated, experiments performed in Jurkat or MA5.8 cell lines suggested that the hexameric TCR complexes (without the CD247 homodimer), exit from the ER independently of CD247 (Dietrich *et al.*, 1999; Sussman *et al.*, 1988) and as the TCR chains were retained in Golgi apparatus, they guessed that the hexameric TCR may be degraded in the lysosome. It is now well known that some unassembled and/or aberrant proteins or proteins that for any reason fail to be transported through

the secretory pathway can be degraded in a proteasome ER-associated degradation (Briant *et al.*, 2015; Tiwari *et al.*, 2001; Werner *et al.*, 1996). Other studies have found that certain TCR chains have sequences that makes them susceptible to be degraded this proteasome-dependent mechanism, such as TCRα (Bonifacino, Cosson*, et al.*, 1990), CD3δ (Yang *et al.*, 1998) or CD247 (Wang *et al.*, 2001) (Fig Intro 2). In addition, when these chains are not assembled, they have different stability so TCRα, TCRβ and CD3δ are rapidly degraded whereas CD3γ and CD3ε are more stable and may be accumulated on ER (Wileman *et al.*, 1990). Particularly in the case of CD3δ chain, the protein needs the trimming of mannose residues from asparagine-linked (N-linked) oligosaccharides, then the generation of ubiquitinated membrane-bound intermediates, and the proteasome-dependent removal from the ER membrane (Yang *et al.*, 1998). TCRα was also found to be degraded in a proteasome-dependent manner with ubiquitinated intermediates but not through mannose modifications (Yang *et al.*, 1998), indeed having a 23-amino acid sequence in the carboxyl-terminal that give the specificity for this proteasome ER-proteasome mechanism(Bonifacino, Suzuki*, et al.*, 1990; Minami *et al.*, 1987).

1.3. TCR-immunodeficiencies (TCRID) and revertant somatic mosaicism

Congenital immunodeficiency (ID) disorders affecting several TCR chains, hereafter referred to as TCRID, have been considered during the last 25 years. Due to the crucial role of TCR signalling during T-cell selection in the thymus, mutations in *TCR*, *CD3* or *CD247* genes selectively impair T-cell development (A. V. M. Marin *et al.*, 2015). Deficiency in any of the invariant chains of the TCR causes either severe T-cell lymphopenia as noted in CD3δ or CD3ε deficiency, or mild T-cell lymphopenia as reported for CD3γ or CD247 deficiency (Fig Intro 2) (reviewed in (A. V. M. Marin *et al.*, 2015)) and deficiencies in the only variant chain described until the date, TCRα, only two cases in the literature, debut with selective αβ T-cell lymphopenia (Morgan *et al.*, 2011). In addition to the complete defects, several partial defects have also been described (reviewed in (Garcillan *et al.*, 2015)). The spectrum may vary from the most severe cases where T lymphocytes are undetectable in peripheral blood, such as mutations in *CD3D* or *CD3E* that lead to the total loss of the protein and cause very severe recurrent infections that threaten life at very early age (Dadi *et al.*, 2003; Firtina *et al.*, 2017; Takada *et al.*, 2005), to those with mere autoimmunity symptoms, like many cases of mutations in *CD3G* (Arnaiz-Villena *et al.*, 1992; Gokturk *et al.*, 2014; Regueiro *et al.*, 1986). Depending on the type of TCRID, the defect could debut at different levels beyong the T-cell generation, maturation or function (A. V. M. Marin *et al.*, 2015). The TCR, as a protein complex, requires specific structure and certain conformational changes to transmit the binding signal of an antigen presented in an MHC complex to the machinery of the cell to develop the proper T-cell response (Schamel *et al.*, 2019) so alterations in any TCR chain may affect T-cell function and compromise the immune response. The more frequent clinical features of TCRID patients, from the severe combined immunodeficiency (SCID) to combined ID according to the severity of the symptoms, are recurrent respiratory infections, otitis, candidiasis, diarrhea, failure to thrive, and sometimes autoimmune phenomena in the first year of life (A. V. M. Marin *et al.*, 2015). Haploidentical stem cell transplantation (HSCT) is usually prescribed and the sooner the treatment, the better survival rate (Castagnoli *et al.*, 2019). As mentioned, autoimmune phenomena have been described in several TCRID patients, mainly when T-cells are present, like in CD3γ- or TCRα-deficient patients (Arnaiz-Villena *et al.*, 1992; Gokturk *et al.*, 2014; Morgan *et al.*, 2011), for which the penetrance may be incomplete.

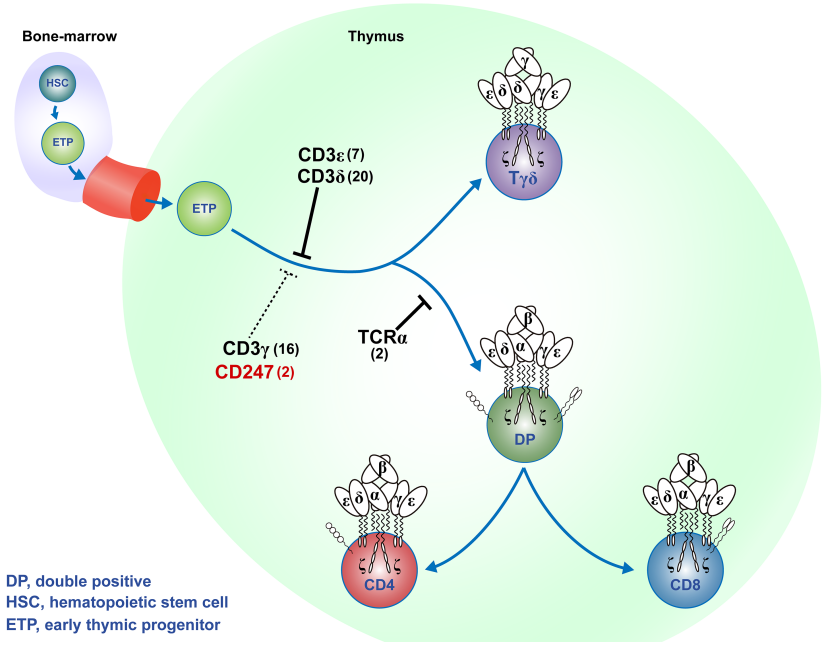

Figure Intro 2. Impact of mutations causing complete TCRID on human αβ and γδ T-cell development, summarizing the data reviewed in previous papers (Garcillan *et al.*, 2015; A. V. M. Marin *et al.*, 2015). Numbers indicate the approximated number of patients described with total protein loss due to mutations reported in the literature. Until the date, no deficiencies have been reported for the genes codifying of TCRβ, TCRγ or TCRδ. ζ refers to CD247, both names can be used equally. HSC, hematopoietic stem cell; ETC, early thymic progenitor; DN, double negative ($CD4^{-}CD8^{-}$); DP, double positive ($CD4^{+}CD8^{+}$).

Regarding CD247, two deficient patients due to point mutations have been described so far (Rieux-Laucat *et al.*, 2006; Roberts *et al.*, 2007). Both patients showed moderate T-cell lymphopenia and strongly reduced surface TCR expression and interestingly, in both cases, two populations of T-cells were identified, a major population with strikingly low levels of surface TCR and a minor population with almost normal levels. Rieux-Laucat and cols. reported that the T-cells with higher levels of TCR expression arose by somatic mutations in *CD247* that partially reverted the inactivating germ-line mutation, allowing higher surface expression of poorly functional TCR complexes and attending to the T-cell phenotype, somatic mutations may have also occurred for the second patient, but no molecular analysis was reported (Roberts *et al.*, 2007). Somatic mosaicism arises when specific cells within a developing organism mutate to result in two or more cell populations with distinct genotypes (Campbell *et al.*, 2015), a phenomena that is very common primary immunodeficiencies such as Wiskott-Aldrich syndrome, X-linked SCID or Adenosine deaminase deficiency, belong others (Davis *et al.*, 2009) (Moncada-Vélez *et al.*, 2011; Speckmann *et al.*, 2008), for which the genetic events can offset the pathogenic effect of the disease but also be neutral or clinically detrimental (Revy *et al.*, 2019). At this point, it was unclear if the presence of somatic mutations was pathognomonic of CD247 deficiency and conferred any benefit or not to the pathology, but it was clear that they have never been observed in other TCRID.

In the Objective 1, we describe an infant born to consanguineous parents with early-onset chronic cytomegalovirus (CMV) infection, SCID and extremely low surface CD3 levels. The study resulted in the diagnosis of a complete CD247 deficiency with mosaicism due to somatic mutations that restored TCR expression and function (A. V. Marin *et al.*, 2017). In the objective 2, we develop a simple and fast diagnostic procedure for TCRID patients, affordable for a basic immunology lab.

1.4. TCRID *in vitro* models

Blood samples from ID patients are often received from abroad and travel long distances at changing temperatures before they reach the diagnostic lab. In such cases it is important to include age-

matched controls that suffer similar shortcomings, so that comparisons can be meaningful. Regarding TCRID patients, they may have no T-cells or have only small number ($T^{-}B^{+}NK^{+}$ or $T^{\pm}B^{+}NK^{+}$), plus the reduced amount of blood (very often less than 5 mL) and the travelling issue, it is a challenge to obtain enough T-cell number to address the experiments necessary to elaborate the diagnosis and characterize as better as possible the pathology of the patient. The generation of T-cell lines derived from these patients could be hard going but whenever it works, the material can be use indefinitely (A. V. M. Marin *et al.*, 2015). This background correlates with the fact that much of the TCR research has been done with *in vitro* cell lines, most of them derived from Jurkat, or mouse models, but not specifically with TCRID patient cells due to the scarcity and the difficulty of generating cell lines from them. The most studied *in vitro* TCRID model, derived from patient T-cells, has been Herpesvirus Saimiri (HVS) immortalized cell lines from several CD3γ-deficiency patients, for which cell lines reproduced the biology of the original cells and were studied deeply for years (Reine *et al.*, 2011; Rodriguez-Gallego *et al.*, 1996; Sun *et al.*, 1997; Torres *et al.*, 2003). Some results that have not been confirmed in TCRID derived cell lines are how the absence of a unique TCR chain may affect other levels or function (Bonifacino *et al.*, 1989), or the more relevant TCR degradation mechanism when the complex is not assembled correctly. For example, the only reference of CD247 deficiency *in vitro* model is the murine MA5.8 cell line (Geisler *et al.*, 1989). In the Objective 3, we present a cell culture protocol to generate stable human T-cell lines that was developed to obtain CD247-haploinsufficient and -deficient cell lines from the CD247-deficient patient and family members.

With this background, in the Objective 4 we were focused into the study of the impact of reduced or absent amounts of CD247 on the TCR complex, from the synthesis of TCR chains to the assembling and trafficking process of the TCR complex, using the stable Human T-lymphotropic virus type 1 (HTLV-1) immortalized cell lines generated in the Objective 3. The knowledge about the TCR biology in human by using these TCRID as models may shed some light to the management of this immunodeficiencies cases with very bad prognosis and be the basic for new therapies for diseases mediated by T-cells.

2. OBJECTIVES

The human αβ TCR is composed of one variable heterodimer (TCRαβ), two invariant heterodimers (CD3εγ and CD3εδ) and one invariant homodimer (CD247, also called ζζ). It has a crucial role during T-cell selection and activation, so that mutations in the genes codifying for TCR chains cause immunodeficiency disease (TCRID) of varying severity depending on the affected protein, which requires early diagnosis. TCRID cases are extremely rare but valuable models to understand human TCR biology, considering that mouse models or human genetically modified tumoral cell lines do not fully recapitulate the behaviour of the human TCR.

2.1. **Objective 1.** To characterize a congenital CD247 ID

2.2. **Objective 2.** To improve the diagnosis of TCRID

2.3. **Objective 3.** To generate patient-derived CD247-deficient and -haploinsufficient T-cell lines

2.4. **Objective 4.** To study TCR dynamics in such T-cell lines

3. MATERIALS AND METHODS

3.1. Objective 1

3.1.1. Case report

The case has been reported in full previously (A. V. Marin *et al.*, 2017; Vales-Gomez *et al.*, 2016). Briefly, the patient was a Turkish girl born from consanguineous parents, healthy until 2 months of age, admitted for sepsis because of a 10-day fever after routine vaccination (DPT-polio/Hib and BCG). Immunoglobulin levels were normal. She showed symptoms of hemophagocytic lymphohistiocytosis, and therefore she was started on steroids. She was diagnosed of CMV infection and received intravenous ganciclovir and intravenous immunoglobulin. Lymphocyte subsets determined 0,5% of T lymphocytes, of which 0.3% were helper and 0.1% cytotoxic, 23% of B cells and 36% of NK-cells. T lymphocyte activation in response to phytohemagglutinin (PHA) was extremely low. She was diagnosed for our research group at 11 months of age of TCRID due to a mutation in *CD247*. At 19 months of age, maternal haploidentical HSCT was performed after fully HLA-compatible donor screening failed within and outside her family. The first week after HSCT CMV reactivation was detected but maintained under control. Myeloid and platelet engraftment were detected two weeks after HSCT and one year after 97% of donor chimerism was reached. During this time, she suffered acute graft vs host disease complicated with pneumonia, pulmonary hypertension and renal failure, for which she was treated with immunosuppressant and symptomatic drugs and cares. At 13 months after HSCT, she died of respiratory failure despite intensive care. Regarding the family members, certain autoimmune disorder markers were studied and result to be negative. The study was conducted according to the principles expressed in the Declaration of Helsinki and approved by the Institutional Research Ethics Committees of the hospitals involved. All participants or their guardians provided informed consent for the collection of samples and subsequent analyses.

3.1.2. PBMC isolation and culture

Peripheral blood mononuclear cells (PBMC) from the patient, her family and healthy controls (age-matched whenever possible) were isolated by centrifugation on a Ficoll-Paque PLUS (GE Healthcare) gradient. Polyclonal T-cell lines were generated by stimulation at day 0 with 1 μg/mL PHA (Sigma-Aldrich), and co-culture with irradiated allogeneic feeder cells weekly (PBMC and Epstein-Barr virus-transformed B cells, 40 and 65 Gy, respectively) at 1:2 ratio in IMDM medium (GE Healthcare) supplemented with 40 IU/mL recombinant human interleukin-2 (IL-2, provided by Craig W. Reynolds, Frederick Cancer Research and Development Center, NCI, NIH, Frederick, Maryland, USA), 10% AB^+ human serum, and 1% L-glutamine and Antibiotic-Antimycotic (Gibco). Cell growth was calculated weekly as the ratio of recovered vs seeded cells, and long-term growth plots were estimated as projections thereof.

3.1.3. Immunophenotype

Extracellular multiparametric flow cytometry was performed by standard protocols using monoclonal antibodies (mAb) against CD3ε (UCHT-1 and S4.1), CD4 (13B8.2), CD45RA (ALB11), CD45RO (UCHL-1) from Beckman Coulter; αβTCR (BMA 031) from Miltenyi Biotec; γδTCR (11F2), CD31 (WM59), CD27 (M-T271), CD56 (B159) and CD8 (RPA-T8) from BD Biosciences. For intracel-

lular staining, cells were fixed with 2% paraformaldehyde and permeabilized with 0.5% saponin as standard procedures, using monoclonal antibodies against CD3ε (UCHT-1) from Beckman Coulter; CD3δ (EP4426), CD3γ (EPR4517) and CD3ε (EPR5361(2)) from Abcam; CD247 (6B10.2) from Biolegend. For unlabeled antibodies, an additional step with phycoerythrin (PE)-conjugated anti-mouse IgG (H+L) from Beckman Coulter or anti-rabbit IgG (H+L) from Life Technologies was performed. Data were acquired with a FACSCalibur flow cytometer (BD Biosciences) and analyzed with FlowJo software (TreeStar).

3.1.4. T-cell function

To analyze CD69 induction as activation marker after TCR engagement, $0.2x10^6$ PBMC were plated in flat-bottom 96-well plates and stimulated for 24 hours with 10 μg/mL of plastic-coated anti-CD3εδεγ mAb (UCHT-1 from BD Biosciences). CD69 induction was analyzed by flow cytometry with anti-CD69 (L-78 from BD Biosciences). Proliferation was measured by dilution of the cell tracer carboxyfluorescein diacetate succinimidyl ester (CFSE from Sigma Aldrich). Briefly, cells were stained with 1 μM CFSE and stimulated with 1 μg/mL UCHT-1 (eBioscience) for 5 days. Phosphorylation of ZAP-70 and ERK proteins was determined by intracellular flow cytometry after stimulation of 0.3x106 cultured cells with 20 μg/mL anti-CD3ε mAb (OKT3 from eBioscience) at 4ºC for 30 minutes cross-linked with 10 μg/mL goat F(ab')2 anti-mouse Ig (H + L) (Beckman Coulter) at 37 °C for 10 min. Phosphorylated (p) proteins were detected by intracellular flow cytometry with rabbit antibodies against pERK (Thr202/Tyr204) and pZAP-70 (Tyr319) / pSyk (Tyr352) from Cell Signaling. A second step with PE-labeled anti-rabbit antibody (Life Technologies) was performed.

3.1.5. TCRβ clonality

Clonality at the TCRβ locus was studied using a commercial kit (Master Diagnostica, Granada, Spain, EC-certified for clinical use), which amplifies genomic TCR VβJβ rearrangements using two specific primers for conserved V and J flanking regions. Polyclonal (healthy donor) control DNA was included for reference. Amplimers were separated and analyzed in an ABI Prism Genetic Analyzer 3110 using GeneMapper V 4.0 from Applied Biosystems.

3.1.6. *CD3* and *CD247* sequence analysis

Genomic DNA and RNA were obtained from peripheral blood or cultured $CD3^{low}$ or $CD3^{high}$ patient T-cells. Primers for *CD3G*, *CD3E* and *CD3D* have previously been described in (Gil *et al.*, 2011; Recio *et al.*, 2007). CD247/ζ cDNA was amplified using specific exon 1-flanking primers (Forward: 5' ACACCCCAAACCCTCAAACCTC 3'; Reverse: 5' AGGAGGGCAGGATTTGAAGGAG 3') and PCR products were sequenced. For CD247 cloning, cDNA was amplified by PCR using specific primers (Forward: 5' GGAGATCTCCACAGTCCTCCACTTCCTG 3' Reverse: 5' GATCCGCGGCCGCA TAGGAAGGCTTTAGCATGCC 3'). DNA fragments were cloned into pJET 1.2 plasmid (CloneJET PCR Cloning Kit, Life Technologies) and transformed into DH5α E. coli strain. Colonies containing recombinant plasmids were also sequenced. *CD247* haplotypes were determined by analysis of four Sequence Tag Sites in the genetic interval that contains the CD247 gene on chromosome 1q24.2, essentially as described in (Recio *et al.*, 2007).

3.1.7. Western blot

Cells were lysed in buffer containing 0.5% Brij96v; 50 µg of cell lysate were resolved by SDS-PAGE, transferred into Polyvinylidene Fluoride (PVDF) membranes and developed with anti α-tubulin (B5-1-2 clone, Sigma Aldrich) and the rabbit anti-CD247 448 antiserum (specific for the last 34 amino acids of its C-terminal region), kindly provided by Balbino Alarcón, Centro de Biología Molecular Severo Ochoa, UAM-CSIC, Madrid, Spain and previously described (San Jose *et al.*, 1998). Blots were visualized using an Odyssey infrared imaging system and quantified using Image Studio software (both from LI-COR Biosciences).

3.1.8. Statistical analysis

The two-tailed Student t test or one-way ANOVA with Bonferroni's Multiple Comparison Test were performed (*$p \leq 0.05$; **$p \leq 0.01$; *** $p \leq 0.001$). Error bars represent standard error of the mean (SEM).

3.2. Objective 2

3.2.1. PBMC isolation and immunophenotyping

Healthy donors, carriers and CD247 haploinsufficient and deficient patient cells were isolated as described in the section 4.1.2. Extracellular flow cytometry was performed as described in the section 4.1.3 using anti-CD3 (UCHT-1) PE-Cy7 conjugated antibody. Intracellular flow cytometry was performed using Foxp3/Transcription Factor kit from eBioscience™, using monoclonal antibodies against CD3 (UCHT-1) conjugated with FITC from Beckman Coulter; unlabeled CD3δ (EP4426), CD3γ (EPR4517) and CD3ε (EPR5361(2)) from Abcam; CD247 (H146-968) conjugated with AF488 from Thermo Fisher Scientific was used instead of the 6B10.2 clone. For unlabeled antibodies, an additional step with allophycocyanin (APC)-conjugated anti-rabbit IgG (H+L) from Invitrogen (AB_429727) was performed. Data were acquired with a FACSCalibur flow cytometer (BD Biosciences) and analysed with FlowJo software (TreeStar). Statistical significance was studied as indicated in the section 4.1.8 with two-tailed Student approximation.

3.3. Objective 3

3.3.1. Generation of human T-lymphotropic virus type 1 (HTLV-1) cell lines

Healthy donors, carriers and CD247-haploinssuficient or -deficient patient cells expanded with the allogeneic system described in the section 4.1.2 were stimulated with 10 µg/mL PHA from Phaseolus vulgaris (only at day 0) from Sigma-Aldrich (St Louis, Mo) for 24 hours and co-cultured with irradiated (150 Gy) HTLV-1-producing cell line (MT2) at 1:1 ratio in RPMI 1640 medium from Lonza (Switzerland), supplemented with 100 IU/mL recombinant interleukin-2 (rIL-2) (provided by Craig W. Reynolds, Frederick Cancer Research and Development Center, NCI, NIH, Frederick, Maryland, USA), 10% fetal bovine serum and 1% L-glutamine and antibiotics-antimycotic from Life Technologies (Carlsbad, Calif). After 8 weeks, CD4 marker was checked on cell lines by flow cytometry.

3.3.2. Immunophenotype of cell lines

Extracellular flow cytometry was performed as described in section 4.1.3, using mAb against CD3ε (UCHT-1 and OKT-3). Intracellular flow cytometry was performed as described in section 4.2.1. Data

were acquired with a FACSCalibur flow cytometer (BD Biosciences) and analyzed with FlowJo software (TreeStar). Statistical significance was studied as indicated in the section 4.1.8 with one-way ANOVA approximation.

3.4. Objective 4

3.4.1. Western blot and Immunoprecipitation (IP)

To generate whole-cell lysates, cells were lysed in buffer containing 0.5% Brij96v. 80-140 µg of WCL were resolved by 15% SDS-PAGE, transferred into polyvinylidene fluoride membranes, blocked using ½ of Odyssey Blocking Buffer in PBS (from LI-COR Biosciences, Lincoln, Neb) and developed with primary rabbit antibodies against CD3δ (EP4426), CD3γ (EPR4517) and CD3ε (EPR5361(2)) from Abcam; CD247 antiserum (448) (specific for the last 34 amino acids of its C-terminal region), kindly provided by Balbino Alarcón, Centro de Biología Molecular Severo Ochoa, UAM-CSIC, Madrid, Spain; TCRβ Antibody (H-197) and TCRα Antibody (H-142) from Santa Cruz Biotechnology (Dallas, TX); and mouse antibody against α-tubulin (DM1A) from Thermo Fisher Scientific. Secondary antibodies goat anti-mouse IgG (H+L) Highly Cross-Adsorbed Secondary Antibody Alexa Fluor Plus 680 (A32729) and goat anti-rabbit IgG (H+L) Highly Cross-Adsorbed Secondary Antibody Alexa Fluor Plus 800 (A32735) were used, both from Thermo Fischer Scientific. Blots were visualized using an Odyssey infrared imaging system and analyzed using Image Studio software (both from LI-COR Biosciences, Lincoln, Neb). Molecular weight estimation was calculated using a Protein Ladder (Spectra™ Multicolor Broad Range Protein Ladder from Thermo Fisher Scientific) to construct a standard curve of log molecular weight versus relative migration distance, obtaining always R^2>0,99.

For the IP, protocol recommended by Dynabeads™ Protein G (Thermo Fisher Scientific) was used. In brief, UCHT-1 antibody was incubated with the Dynabeads (2 µg of antibody for each 10 µL of Dynabeads into 200 µL of PBS-Tween 0.02% or IP-buffer) for 30 minutes at room temperature. After washing the beads twice with IP-buffer, 1-2 mg of WCL of each cell line were incubated with the antibody-coated Dynabeads for 2 hours at 4ºC. After washing the target antigen immobilized in the Dynabeads three times, the antigen was delivered by incubating them into lysis buffer containing 0.5% Brij96v for 5 minutes at 95ºC, and Dynabeads were removed from the mix using the magnet. For each cell line and immunoblotting, 80 µg of whole-cell lysate (Lysate), slightly increase amount of whole-cell lysate (80-140 µg, enriched whole-cell lysate or E. lys) and IP products were resolved and revealed as previously indicated.

3.4.2. Confocal microscopy of TCR components and colocalization

Cells were fixed and permeabilized using using eBioscience™ Foxp3 / Transcription Factor Staining Buffer Set, blocked with human IgG and goat serum (1/100 both) and stained with primary antibodies against CD3δ (EP4426), CD3γ (EPR4517), CD3ε (EPR5361(2)) and Calnexin (EPR3633(2)) from Abcam; CD247 antiserum (448) from Balbino Alarcón; CD3εδ/εγ (UCHT-1), GM130 (PA1-077), TGN46 (PA1-1069), EEA1 (PA1-063A) and LAMP-1 (PA1-654A) from Thermo Fisher Scientific; and CD71 (M-A712) from BD Bioscience. Secondary antibodies Superclonal anti-Mouse IgG, AF488 (A28175) and Superclonal anti-Rabbit IgG, AF555 (A27039) were used, both from Thermo Fisher Scientific. Slides were mounted into ProLong® Diamond Antifade Mountants with DAPI from

Lifetechnologies (Carlsbad, CA). Images were obtained in the Center for Cytometry and Fluorescence Microscopy of Complutense University of Madrid (Spain) with a Leica TCS SP8 Confocal Microscope and analysed and processed with ImageJ (National Institutes of Health). To study colocalization, from 8-12 Z-planes (aprox. 1 μm each) were analyzed with Pearson's test, obtaining Rcoloc correlation coefficients using Fiji/ImageJ. Statistical significance was studied as indicated in the section 4.1.8 with one-way ANOVA approximation.

3.4.3. Surface TCR recycling and downmodulation after TCR triggering

To assess TCR recycling, cells were cultured in round-bottom 96-well microtiter plates with DMSO as control of vehicle or 5 μg/mL brefeldin-A or BFA (B7651, Sigma-Aldrich). At the time points indicated, cells were washed, stained with mouse antibody against CD3εδ/εγ (UCHT-1) and fixed with 2% paraformaldehyde. The relative CD3εδ/εγ surface expression is expressed as a percentage of the total surface levels in DMSO condition for each cell line. Surface flow cytometry was performed as indicated previously.

To assess TCR down-modulation, cells were cultured in round-bottom 96-well microtiter plates with anti-CD3εδ/εγ mouse antibody (OKT3 from eBioscience) for 30 minutes at 4ºC. Then cells were washed twice and incubated in the presence of 10 μg/mL Goat F(ab')2 Anti-Mouse IgG (H+L) in presence of 100 μM chloroquine or CHL (C6628, Sigma-Aldrich) to avoid any degradation of internalized TCR. for the indicated time points. Surface expression was revealed using goat anti-mouse PE (AB_11063706) antibody (Thermo Fischer Scientific) and normalized for each cell line in non-treated conditions. Some cells from 180 minutes of incubation were fixed, permeabilized, stained and analysed for confocal microscopy, following the protocol indicated previously. The half-life (min) and the rate constant of surface expression decay (K, min^{-1}) were estimated applying a one-phase decay exponential in GraphPad Prism, attending to R-square (R^2) values.

3.4.4. TCR degradation (CHL vs MG132)

To assess the surface TCR levels in conditions of inhibition of protein degradation pathways, cells were cultured in round-bottom 96-well microtiter plates in the presence of DMSO, 10 or 100 μM chloroquine or 10 or 20 μm MG132 (M7449, Sigma-Aldrich) for 180 minutes. Then cells were washed twice with PBS-BSA 2% and stained for CD3εδ/εγ (UCHT-1) and TCRαβ (IP26). Surface flow cytometry was performed as indicated previously. TCR surface expression was relativized to DMSO condition of control cell line. Statistical significance was studied as indicated in the section 4.1.8 with one-way ANOVA approximation.

To study the TCR chains by western blot, cells were cultured in the presence of DMSO, chloroquine (100 μM) or MG132 (10 μm) for 180 minutes. Then cells were washed twice with PBS-BSA 2%, lysed and immunoblots were performed as indicated previously.

4. RESULTS

4.1. **Objective 1.** To characterize a congenital CD247 ID

We first performed a general immunological study by flow cytometry of a peripheral blood sample of the patient at 11 months of age. Comparing with a normal range of healthy donors of similar age, the patient showed low T- and B-cell counts, the last with slightly more abundance of immature cells, and normal NK-cells, neutrophils and eosinophils (Table 1.1). T lymphocytes were sorted by CD3 surface expression, for which 44% of lymphocytes showed almost undetectable CD3 surface levels ($CD3^{low}$) and 0.16% of them levels similar to carriers ($CD3^{high}$).

Table 1.1. Immunological phenotype

	Patient (11 mo)		**Normal range (11-15 mo)**
Lymphocytes (cells/mm^3 (%))	**3000**		3200-12300
	$CD3\varepsilon^{low}$	$CD3\varepsilon^{high}$	
T ($CD3^+$)	**1315 (44)**	**5** (**0.16**)	2400-8300 (56-87)
$CD4^+$	**66** (**5**)	**3** (57)	1300-7100 (25-86)
$CD8^+$	1183 (**90**)	**2** (29)	400-4100 (7-58)
DN ($CD4^-CD8^-$)	66 (**5**)	**0.7** (**14**)	12-140 (0.42-2)
$TCR\gamma\delta^+$	**7** (**0.5**)	**0** (**0**)	70-630 (1-10)
CD4/CD8 ratio	**0.06**	**1.5**	1.7-3.2
B ($CD19^+$)*	**75** (3)		110–7700 (3-77)
$CD27^-$ IgD^+	**68** (91)		100-7407 (91-96)
$CD27^+$ IgD^+	**0.8** (**1**)		2-316 (1.6-4.1)
$CD27^+$ IgD^-	1.5 (**2**)		0-154 (0.1-1.9)
$CD27^-$ IgD^-	4.5 (**6**)		1-185 (0.9-2.1)
NK ($CD56^+$ $CD16^+$)	1020 (34)		71-3500 (1-64)
Neutrophils (cell/mm^3)	1500		1500-8000
Eosinophils* (cell/mm^3)	200		40-800

Bold = out of range. *B cells and eosinophils were determined at 13 and 15 mo respectively. Normal range updated from (Aksu *et al.*, 2006; Ikinciogullari *et al.*, 2004; Morbach *et al.*, 2010; Schatorje *et al.*, 2012). *Mo*, months. Table adapted from (A. V. Marin *et al.*, 2017).

DNA from the patient's PBMC (almost totally $CD3^{low}$ cells) and from *in vitro* expanded T lymphocytes (enriched in $CD3^{high}$ cells) was used to sequence the *CD247* and no other TCR chain genes, because the presence of some lymphocytes with almost normal levels of surface CD3 was previously described in two CD247-deficient patients (Rieux-Laucat *et al.*, 2006; Roberts *et al.*, 2007). DNA sequencing revealed a homozygous T-to-C mutation at position +2 of exon 1 of *CD247* (NCBI/ClinVar: rs672601318) which causes loss of the initiation codon and therefore prevents translation (Fig 1.1, A and B). The sequencing of expanded patient T lymphocytes revealed two independent somatic mutations at or near the germ-line mutation: a reversion (c.2T>C>T) and a second-site mutation (c.-8A>T) which generates an alternative in-frame initiation codon, three codons upstream of the original ATG (Fig 1.1, A). The patient's parents and four additional family members were asymptomatic but heterozygous for the mutation (Fig 1.1, C).

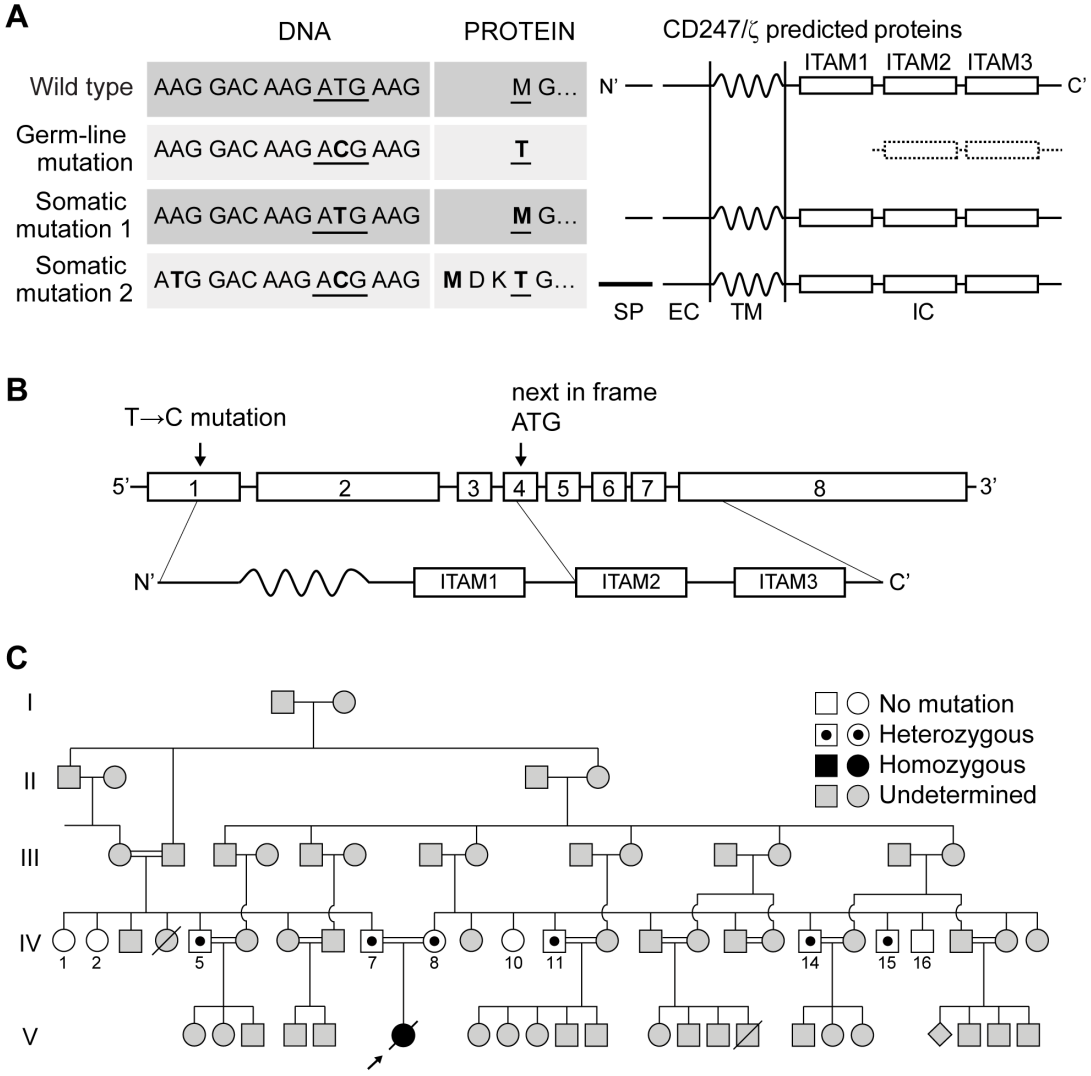

Figure 1.1. CD247 deficiency due to a homozygous mutation. **A**, Mutations identified in the patient DNA, including the germline mutation (NCBI/ClinVar: rs672601318, NM_000734.3:c.2T>C and NG_007384.1:g.5146T>C in exon 1) and predicted proteins of each variant. **B**, CD247 gene and protein, including the germline mutation and the next in-frame ATG. **C**, pedigree for studied individuals. *Circles*, *squares*, and *diamonds* indicate females, males, or unknown sex, respectively. Figure adapted from (A. V. Marin *et al.*, 2017).

To study T lymphocytes in depth, we gated lymphocytes using regular markers of T-cells such as CD4, CD8 and TCRγδ and evaluated within them the CD3 expression in the patient, carriers and healthy donors by flow cytometry (Fig 1.2, A). Considering both CD4 and CD8^{bright} αβ T-cells, surface CD3 expression was markedly reduced in both αβ and γδ T-cells (Fig 1.2, B). The quantification of total CD3 surface expression indicated that carriers showed an important CD3 surface expression defect (around 50% MFI relative to HDs) and was almost undetectable in most of the patient T-cells (Fig 1.2, C). Interestingly, surface CD3 expression in mutation carriers was reduced consistently, revealing a clear correlation between surface CD3 and *CD247* genotype, which was useful for diagnosis and genetic counseling.

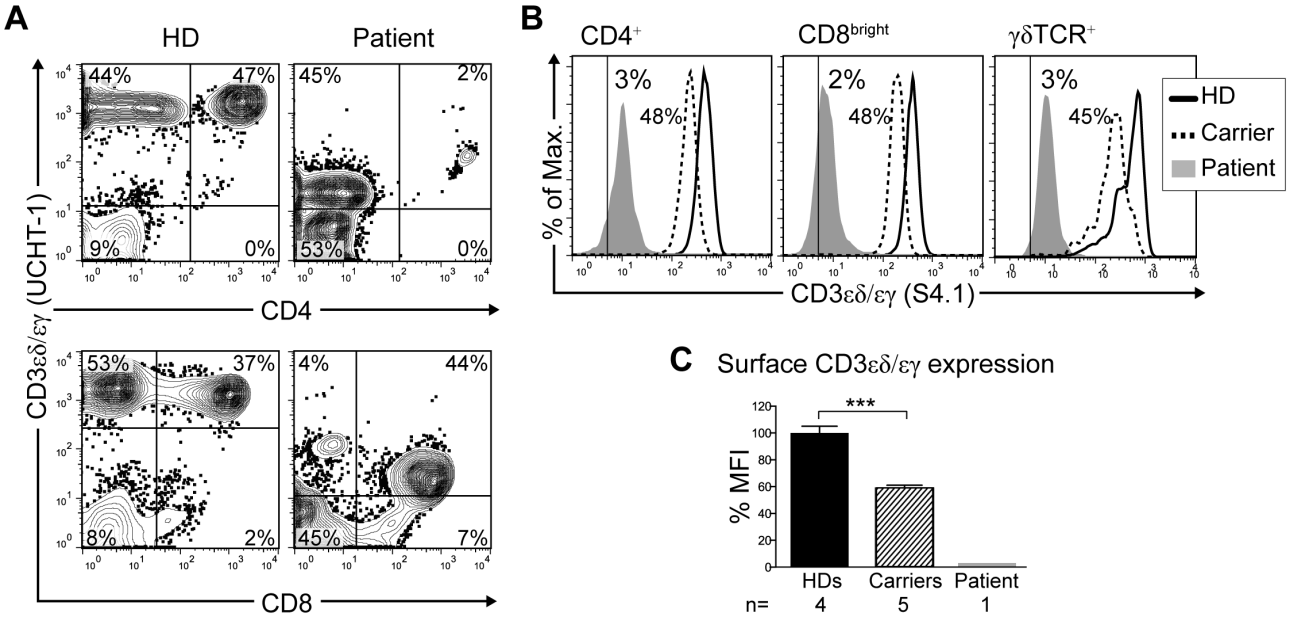

Figure 1.2. Patient extracellular TCR characterization. A, PBMC phenotype of CD3ε *vs* CD4 or CD8 distribution in patient and HD. **B**, Surface CD3ε expression within the indicated subsets in patient, carrier and HD. Numbers indicate % mean fluorescence intensity (MFI) relative to controls. **C**, Quantification of the expression of CD3ε of each group relative to healthy donors (HDs). Two-tailed Student t test was performed (*** $p \leq 0.001$). Error bars represent standard error of the mean (SEM). Figure adapted from (A. V. Marin *et al.*, 2017).

To confirm the CD247 protein defect, we set up a procedure of intracellular double stainings for CD3δ *vs* CD247 and CD3γ *vs* CD3, respectively (Fig 1.3, A), observing a selective and complete defect of CD247 in the patient lymphocytes. These and additional results were used to stablish a diagnostic procedure of TCRID patients and carriers (see Objective 2). Notably, a few T-cells in the patient expressed intracellular CD247 (0,2%), which was compatible with the presence of the somatic mutations detected by sequencing (Fig 1.1, A). To confirm phenomena, T-cells from the patient were cultured in allogeneic condition and patient CD3ε^{high} T-cells became prominent (Fig 1.4). Flow cytometry-sorting and CD247 western blot analysis confirmed that the patient's CD3ε^{high} T-cells had recovered CD247 expression and that the predicted truncated protein of the germline *CD247* mutation was not detected (Fig 1.3, B).

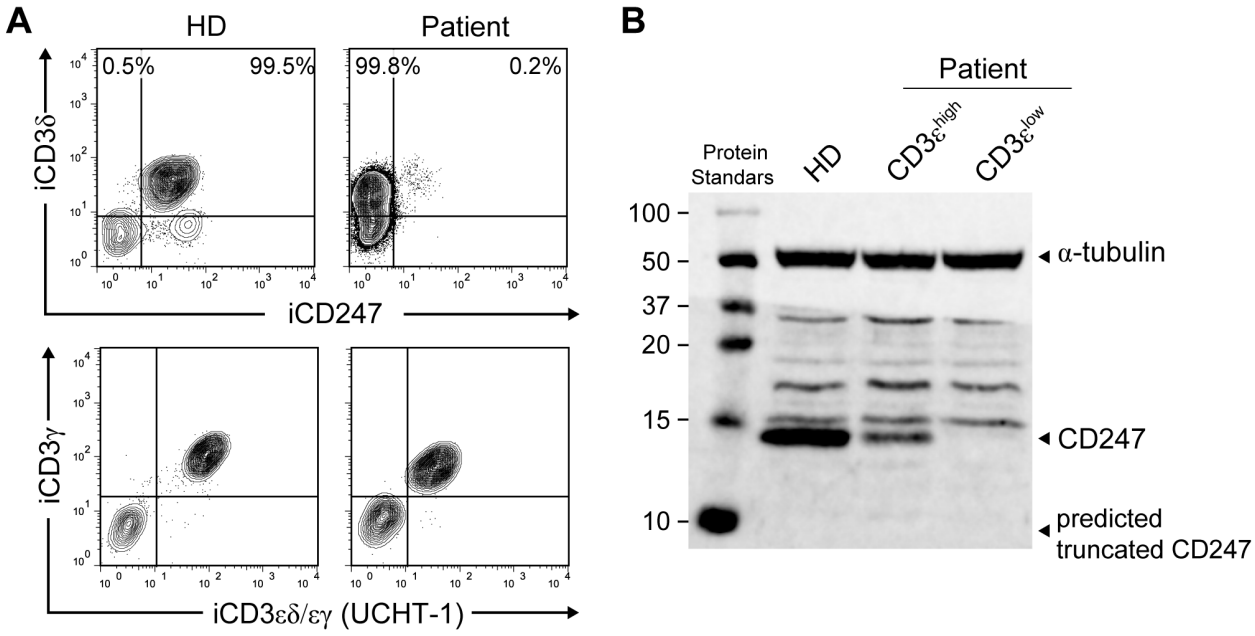

Figure 1.3. Patient intracellular TCR characterization. A, Intracellular (i) double stainings were performed of PBMC using the indicated antibodies. Numbers indicate % iCD247^{-} or iCD247^{+} in iCD3δ^{+} (T) cells. **B**, Sorted T-cells of patient, CD3^{low} and CD3^{high}, and healthy donor (HD) were immunoblotted for which α-tubulin, CD247 and predicted truncated CD247 proteins are indicated with narrows. Protein standards bands are indicated at the left of the blot. Figure adapted from (A. V. Marin *et al.*, 2017).

As indicated previously, cell culturing in allogeneic conditions was required to expand CD3ε^{high} cells from the patient that became prominent after 50 days of culturing until they reached a balance of around 50% of presence in the culture with the CD3ε^{low} patient cells (Fig 1.4). These cultures were necessary to the generation of stable T-cell lines used in the Objective 3.

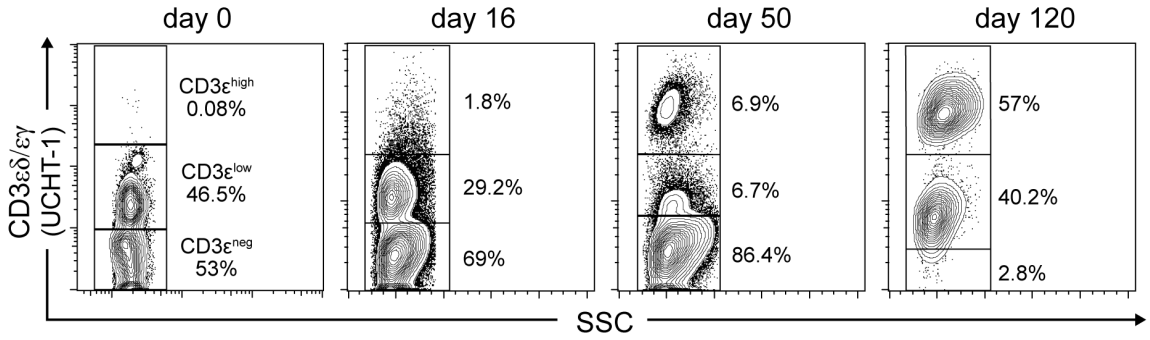

Figure 1.4. Patient *in vitro* T-cell growth and phenotype. Surface CD3 expression in cultured T-cells with gates and % for CD3ε^{neg}, CD3ε^{low}, and CD3ε^{high} subpopulations at different time points. *SSC*, Side scatter. Figure adapted from (A. V. Marin *et al.*, 2017).

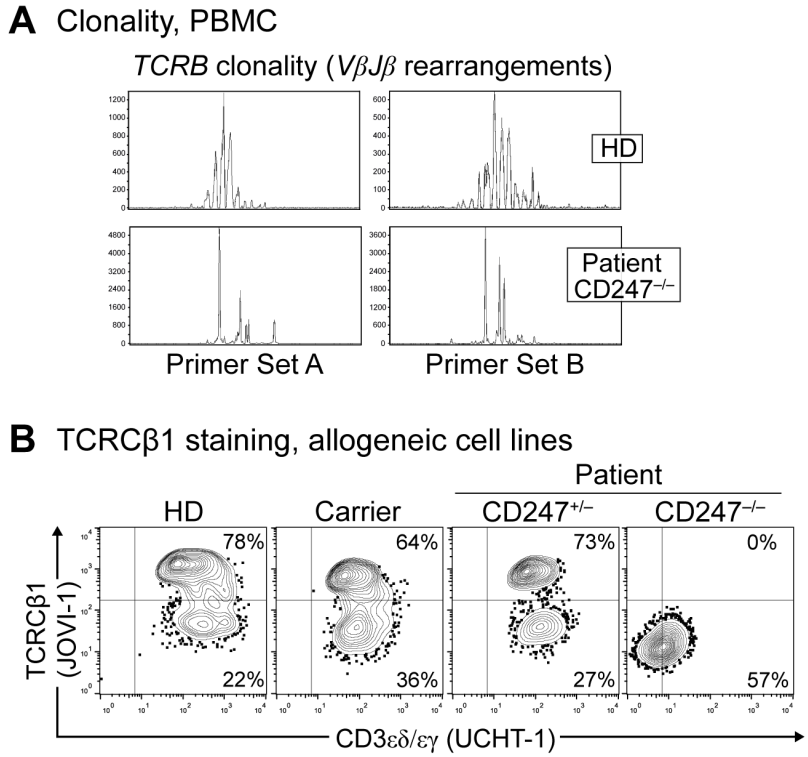

Figure 1.5. Patient T-cell repertoire characterization. A, TCRβ clonality was studied in HD and patient PBMC (99.8% CD247$^{-/-}$) using two primer sets as described in Materials and Methods section. **B**, TCRCβ1 *vs* CD3εδ/εγ staining was studied in HD, a carrier and CD247$^{+/-}$ or CD247$^{-/-}$ patient allogeneic T-cell lines, using JOVI-1 and UCHT-1 clones, respectively. Figure adapted from (A. V. Marin *et al.*, 2017).

To understand the origin of the CD3ε^{low} and CD3ε^{high} cells, we looked for the clonality within peripheral blood (most of them CD3^{low}) or *in vitro* cultured cells (CD3ε^{low} or CD3ε^{high}). Using cDNA and two primer sets from total PBMC, the peaks indicated that the patient presented poor TCRVβ repertoire comparing to HD (Fig 1.5, A). To evaluate the clonality of the revertant T-cells, a surface staining was performed with JOVI-1 clone, a monoclonal mouse antibody that detects one of the two constants domains (TCRCβ1) that a TCRβ can be. We could detect TCRCβ1^{+} and TCRCβ1^{neg} cell in the revertant T-cell culture (patient, CD247$^{+/-}$) but, according to previous peripheral blood T-cell stainings with several antibodies against the variable heterodimer, no TCRαβ at all was detected for the *CD247* germline mutation cell line (patient, CD247$^{-/-}$) (Fig 1.5, B). Our results indicated that patient CD3^{low} cells were oligoclonal and CD3^{high} at least biclonal but further approaches are needed.

Regarding T-cell function, CD69 upregulation and short-term proliferation of primary T-cells after anti-CD3 antibody stimulation was impaired in the patient and reduced in carriers (Fig 1.6, A and B). ZAP-70 and ERK phosphorylation (pZAP-70 and pERK, respectively), was also impaired in CD247-deficient T-cells, while patient revertant T-cells displayed carrier phosphorylation levels (Fig 1.6, C). These results indicate that the reversions could partially rescue TCR signaling *in vitro.* In contrast, the patient's T-cells (both CD3ε^{low} and CD3ε^{high}) readily proliferated when cultured with allogeneic cells and IL-2 (Fig 1.6, D), suggesting that their TCR signaling defect could be overcome if a long-term TCR stimulus together with continuous recombinant human IL-2 supply were present. This is in line with the *in vivo* expansion of the patient´s CD8^{+} T-cells being driven by chronic CMV infection, which in turn would explain their exhaustion and reduced proliferative response *in vitro* compared with their CD4^{+} counterparts. Revertant T-cells were capable of expansion *in vitro* (Fig 1.6, D) and also but less efficiently, *in vivo* (data not shown), where they did not suffice to repopulate the T-cell compartment and consequently produce a clinical benefit.

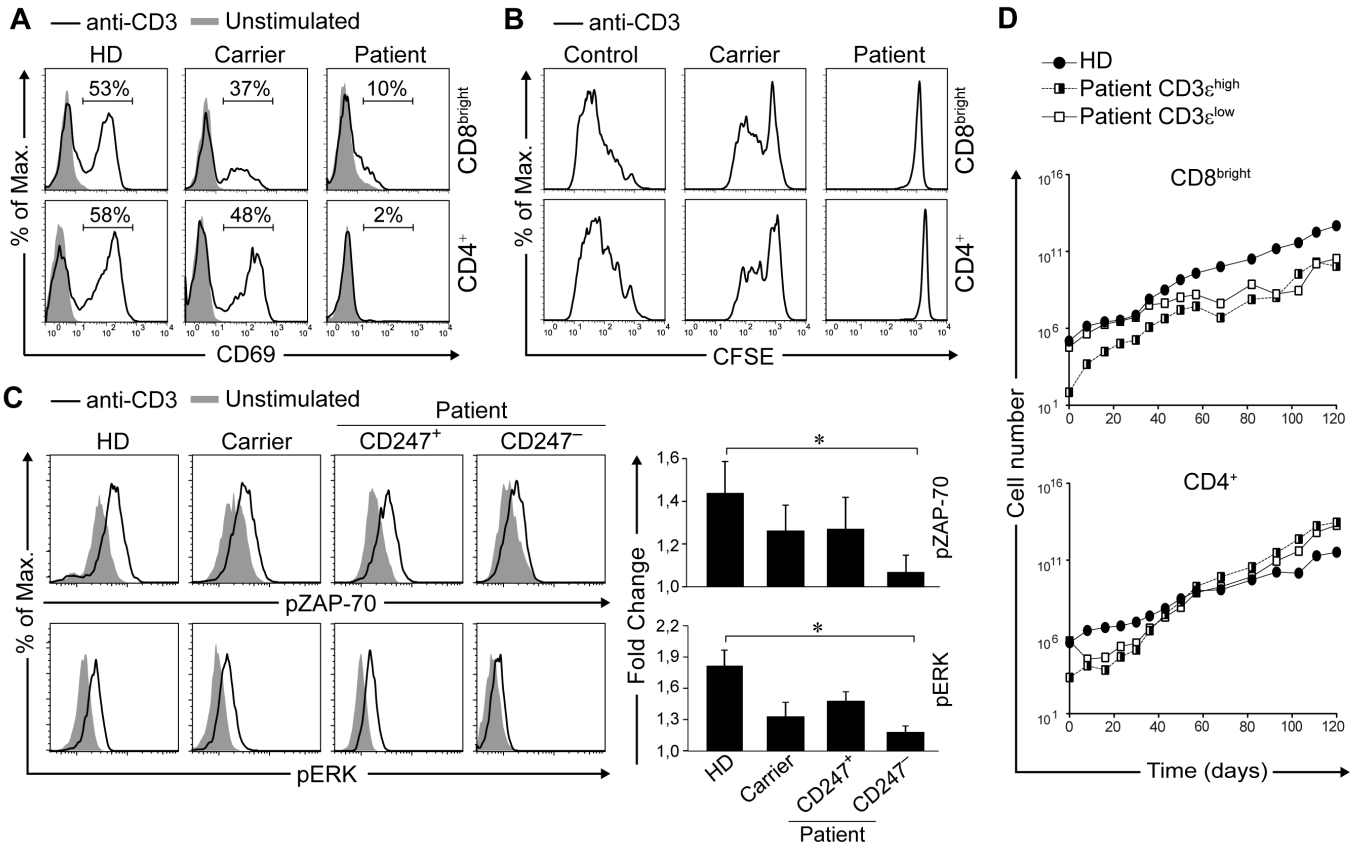

Figure 1.6. Impaired TCR-induced signaling in primary (**A** and **B**) and cultured T-cells (**C** and **D**). % $CD69^+$ cells (**A**) or CFSE dilution (**B**) after stimulation with anti-CD3ε for 24 hours or 5 days, respectively, was studied in HD, carrier and patient (99.8% $CD247^{-/-}$) PBMC. **C**, Representative pZAP-70 and pERK levels after stimulation with anti-CD3ε (left), using intracellular CD247 staining to categorize patient T-cells; MFI + SEM relative to unstimulated cells of 4 independent experiments (right). **D**, T-cell growth in allogeneic cultures, using extracellular CD3 (UCHT-1 clone) staining to categorize patient T-cells. *CFSE*, Carboxyfluorescein diacetate succinimidyl ester; *p-ZAP-70*, phospho-zeta-associated protein; *pERK*, phospho-extracellular signal–regulated kinase. Figure adapted from (A. V. Marin *et al.*, 2017).

Together with two CD247-deficient patients reported in the literature, we prepared a summary figure with the *CD247* mutations and the predicted proteins of each one (Fig 1.7). Our patient was the only one for which the somatic mutations lead to a wild type CD247 protein.

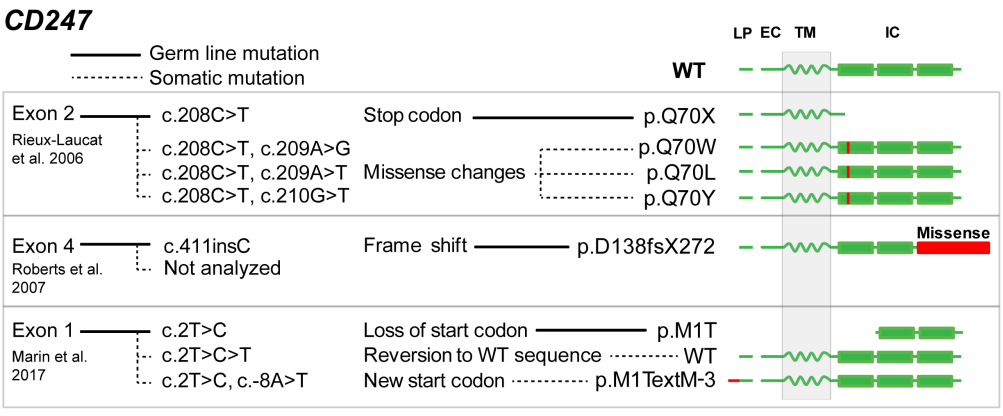

Figure 1.7. Summary of *CD247* germline and somatic mutations. Molecular basis of the 3 reported CD247-deficient patients, 1 patient/box (Exon 2 (Rieux-Laucat *et al.*, 2006), Exon 4 (Roberts *et al.*, 2007) and Exon 1 (A. V. Marin *et al.*, 2017)). *EC*, Extracellular; *IC*, intracellular; *LP*, leader peptide; *TM*, transmembrane; *WT*, wild-type. Figure adapted from (A. V. Marin *et al.*, 2017).

We also summarized the main points of each patient (Table 1.2), highlighting that any of the *CD247* germline mutations was functional and although having received the adequate treatment, the lifespan for these patients could be up to 4-years old in most of the cases, but receiving HSCT seemed to be the better treatment (Rieux-Laucat *et al.*, 2006).

Table 1.2. Comparative clinical and immunological features of CD247-deficient patients.

	Present work, Marin et al 2017	**Rieux-Laucat et al 2006**	**Roberts et al 2007**
Sex	Female	Male	Female
Onset	2 mo	4 mo	4 mo
Age at diagnosis	11 mo	10 mo	11 mo
HSCT (mo)	Haploidentical (19)	Haploidentical (30)	Haploidentical (12, 16)
Present age	†33 mo	13 yº	†4 yº
CMV	+	-	+
Germ line mutation			
Type	Truncation	Truncation	Insertion
cDNA	c.2T>C	c.208C>T	c.411insC
Protein	p.M1T	p.Q70X	p.D138fsX272
Serum Ig levels	High (IgG)	High (IgG, -A, -M, -E)	High (IgG*, -A, -M)
T-cell lymphopenia	Mild	Mild	Mild
CD3ε^{high}			
% of T cells	0.36%	10%	0.6%
Lineage	CD4 and CD8	CD4	CD4 and CD8
Somatic mutations	Yes (2)	Yes (3)	NA
Revertant	Yes	No	NA
Second site	Yes	Yes	NA
Functional	Yes (= carriers)	No	NA
CD3ε^{low}			
% of T cells	99.6%	90.0%	99.4%
CD4/CD8 ratio	Inverted (0.06)	Inverted (0.23)	Inverted (0.85)
Functional	No	No	No

mo (months); y (years); † exitus at; *receiving IVIG; NA (not analyzed); ºAlain Fischer, Paris Descartes Univ. and Rebecca Buckley and Joseph Roberts, Duke Univ., personal communication. Table adapted from (A. V. Marin *et al.*, 2017).

4.2. **Objective 2.** To improve the diagnosis of TCRID

First, extracellular CD3 (specifically a conformational epitope shared by the heterodimers CD3εδ and CD3εγ) expression using UCHT-1 clone revealed a significant partial (55%) or severe (2%) decrease compared to HDs according to the genotype, carriers and patient respectively (Fig 2.1, A). With this result we could confirm nonspecifically that there was an inheritance pattern of TCR expression that affected a component of the complex, and we could identify possible carriers of the defect. To unravel the affected protein, we performed intracellular flow cytometry using two combinations of two antibodies specific for CD247 *vs* CD3δ or CD3εδ/εγ *vs* CD3γ (first direct from mouse, and second unlabelled from rabbit), using commercial buffers from a kit. The results confirmed an undetectable signal of CD247 in the patient but not for other studied TCR chains (Fig 2.1, B). Although CD3εδ/εγ also showed significant decrease in carriers and patient, it was not dramatic as CD247 defect, considering the last one the unique TCR chain affected. Extracellular flow cytometry procedure lasts less than 30 minutes and intracellular up to 2 hours, in contrast to DNA sequencing that could take from 24 hours to several days. Our protocol improves the approximation available to date in terms of time, simplicity and affordability.

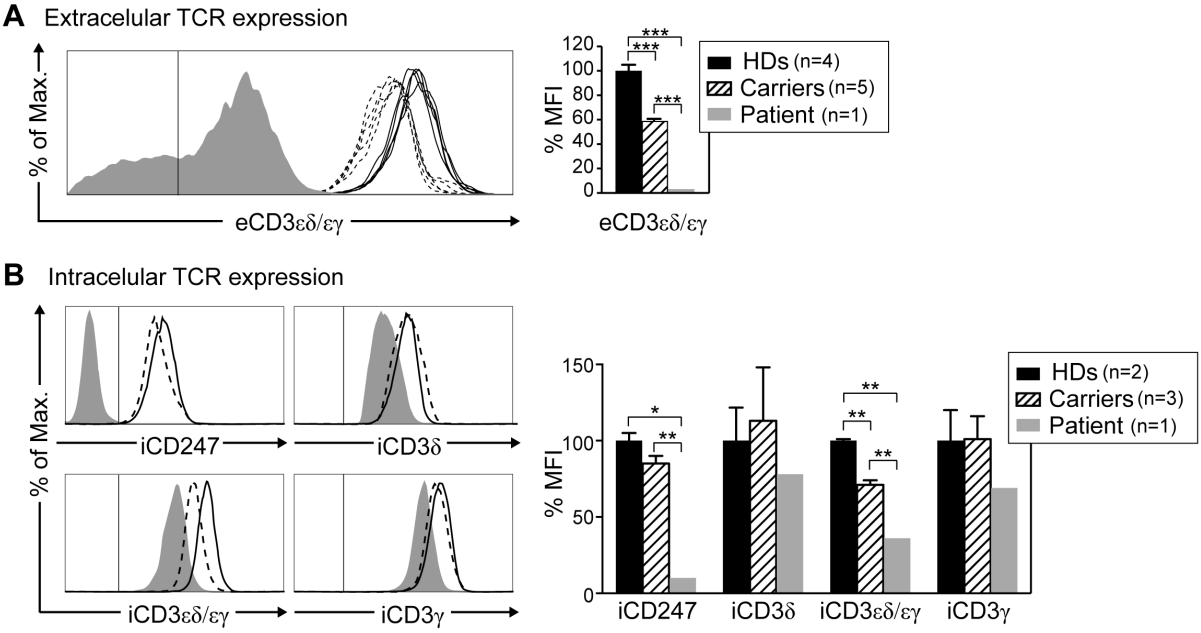

Figure 2.1. TCR chains expression was studied by flow cytometry in the indicated HDs, carrier or patient groups. (**A**) Left, extracellular (e) CD3εδ/εγ histograms of the indicated groups, and right, the geometric MFI resulted from each donor relativized to the HDs group. Note that due to the extremely reduced number of somatic T-cells in patient sample (0.2% of total T-cells), their presence it is not noticed by the peak of the histogram. (**B**) Left, intracellular (i) CD247, CD3δ, CD3εδ/εγ and CD3γ histograms of the indicated groups, and right, the Geo-MFI resulted from each donor relativized to the HDs group. Full materials and methods are indicated in section 4.2.1. Vertical lines indicate isotype control. HDs, healthy donors; n, number of donors. MFI, mean fluorescence intensity. To assess statistical significance, the two-tailed Student t test was performed (*$p \leq 0.05$; **$p \leq 0.01$; ***$p \leq 0.001$). Error bars represent standard error of the mean (SEM).

4.3. **Objective 3.** To generate patient-derived CD247-deficient and -haploinsufficient T-cell lines

CD4 in vitro T-cell lines were generated from HD (Control) or carriers PBMC or sorted CD3high or CD3low patient T-cells from the allogeneic cultures, composing the cell line groups of "control, CD247+/− or CD247−/−". The revertant CD247+/− patient cell line is included in the group of "CD247+/−" by defect.

Surface TCR expression was studied by measuring the expression of the minimal subunit, the heterodimers CD3εδ/εγ using the monoclonal mouse antibodies OKT-3 or UCHT-1 clones (Arnett *et al.*, 2004; Kjer-Nielsen *et al.*, 2004). Surface CD3εδ/εγ was markedly reduced in the cell lines with alterations in CD247 levels (Fig 3.1, A), being almost undetectable in the CD247$^{-/-}$ cell line using OKT-3 clone. The quantification indicated that the surface CD3εδ/εγ levels of the CD247$^{+/-}$ or CD247$^{-/-}$ groups were only 30% or 10% MFI relative to the control group, respec-tively, including the revertant patient cell line in the haploinsufficient group (Fig 3.1, B). The TCR expression defect was more severe than in PBMC (Fig 2.1, A), probably due to the immortalization process.

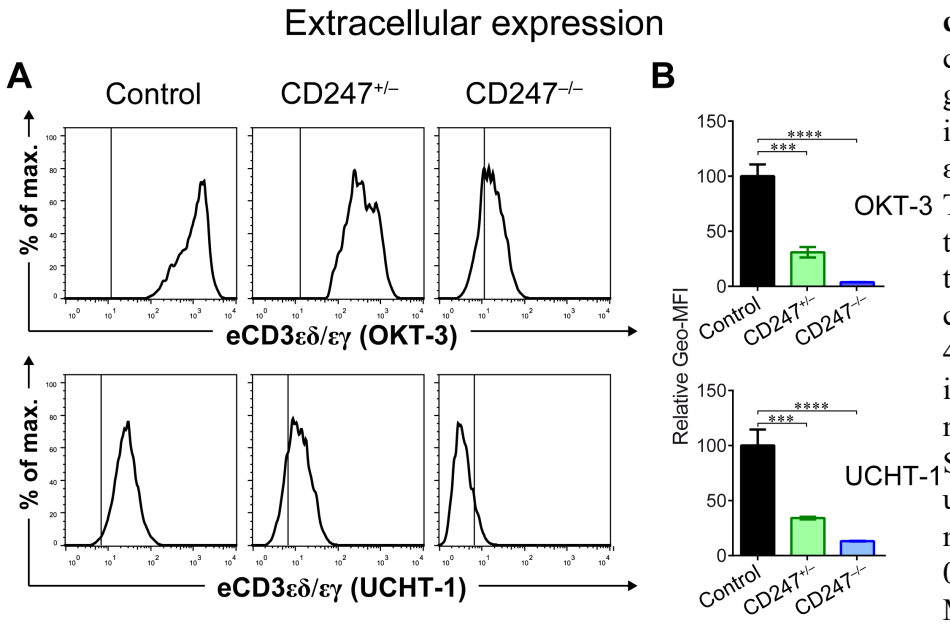

Figure 3.1. Extracellular (e) TCR chains expression was studied by flow cytometry in the indicated cell line groups using antibodies against the invariant chain heterodimers CD3εδ/εγ, OKT-3 and UCHT-1 clones (**A**). The Geo-MFI resulted from each antibody was represented relativized to the control group (**B**). These results correspond with data accumulated of 4 different experiments. Vertical lines indicate isotype control Geo-MFI, geometric mean fluorescence intensity. Statistical significance was assessed using 1-way ANOVA with Bonferroni multiple comparison (*P <0.05, **P < 0.01, ***P < 0.001, ****P < 0.0001). Manuscript in preparation.

Total TCR chains expression was quantified by intracellular cell staining procedures, using mouse monoclonal antibodies against CD3εδ/εγ and CD247 (UCHT-1 and H146-968 clones, respectively), and rabbit monoclonal antibodies against CD3δ, CD3γ and CD3ε (Fig 3.2, A). The CD247 defect was confirmed in our cell lines, reaching around 30% or 10% of the control group in the CD247$^{+/-}$ or CD247$^{-/-}$ groups, respectively, including the revertant patient cell line in the haploinsufficient group (Fig 3.2, B). The 10% for the CD247$^{-/-}$ cell line corresponded with the isotype control levels, that in the cell lines represented higher levels than the same staining for PBMC with only a 2% (Fig 2.1, B). A defect of the expression of CD3δ, CD3γ and CD3ε was also detected for both CD247$^{+/-}$ and CD247$^{-/-}$ groups, that was almost similar in both groups and correlated with a defect in the detection of the heterodimers CD3εδ/εγ with the UCHT-1 antibody (Fig 3.2, B). After having characterize the main levels of TCR chains, we decided to simplify the procedures and work only with one representative cell line of the CD247$^{+/-}$ group, the revertant cell line derived from the CD247-deficient patient.

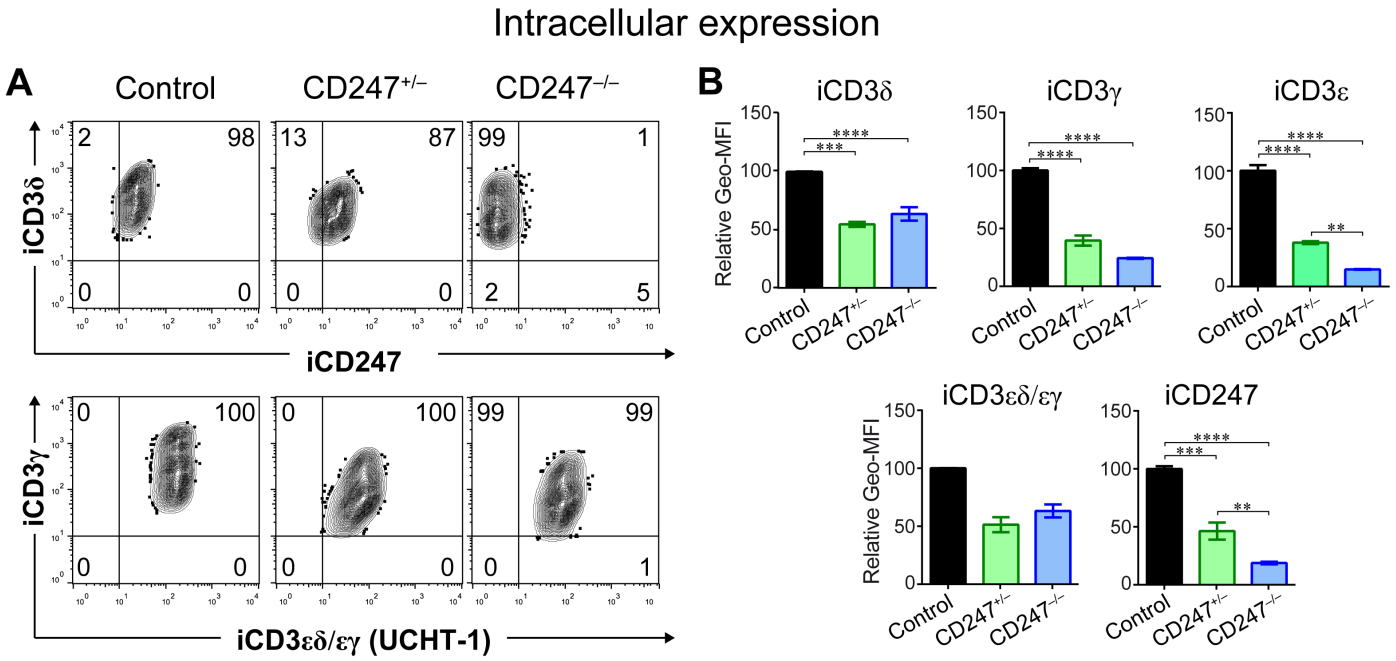

Figure 3.2. Intracellular (i) TCR chains expression was studied by flow cytometry in the indicated cell lines groups using antibodies against CD3δ, CD3γ and CD3ε (EP4426, EPR4517 and EPR5361(2) clones, respectively), CD3εδ/εγ (UCHT-1 clone) and CD247 (H146-968 clone) (**A** and **B**). Goat anti-mouse PE and goat anti-rabbit APC were use as secondary antibodies. These results correspond with data accumulated of 4 different experiments. Numbers on dot plots represent % of cells in each quadrant. Geo-MFI, geometric mean fluorescence intensity. Statistical significance was assessed using 1-way ANOVA with Bonferroni multiple comparison (*P <0.05, **P < 0.01, ***P < 0.001, ****P < 0.0001). Manuscript in preparation.

Then we checked the TCR chains distribution within the cell of CD3δ, CD3γ and CD247 *vs* CD3εδ/εγ by confocal microscopy (Fig 3.3). We observed undetectable signal of CD247 for the CD247$^{-/-}$, as confirmed by flow cytometry, and an area with accumulated signal of the CD3 chains in both CD247$^{+/-}$ and CD247$^{-/-}$ cell lines, suggesting a blockage of the traffic of TCR chains in their way to the cell surface.

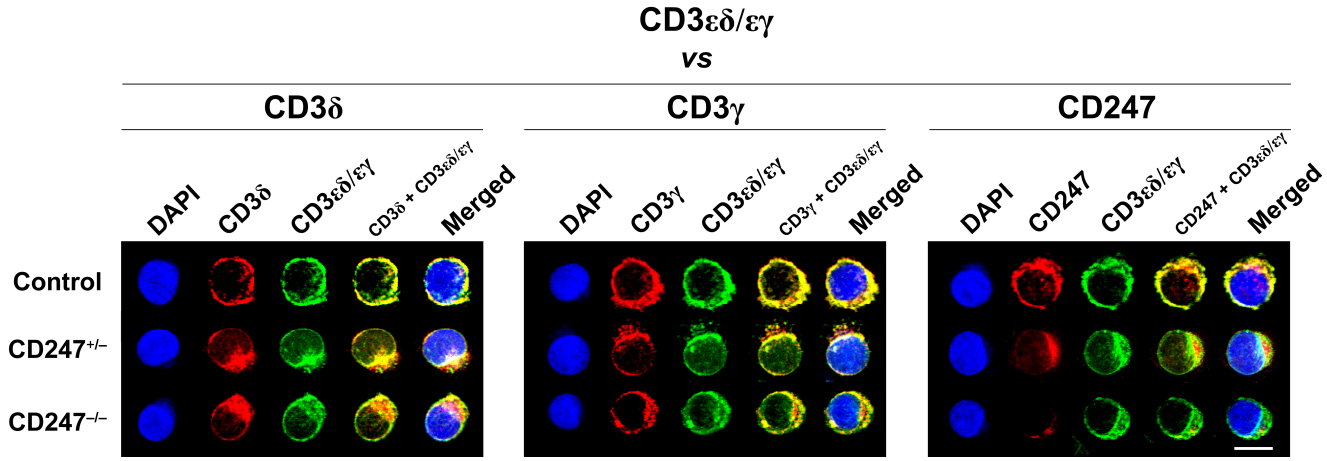

Figure 3.3. Invariant TCR chains distribution by confocal microscopy in one control, the patient revertant haploinsufficient or the CD247-deficient cell lines (CD247$^{+/-}$ or CD247$^{-/-}$, respectively). Total (extracellular and intracellular) TCR chains distribution was studied by confocal microscopy using antibodies against CD3δ, CD3γ and CD247 (EP4426, EPR4517 and 448 clones, respectively, all in red) in combination with CD3εδ/εγ (UCHT-1 clone, green) and DAPI as nuclear marker (blue). Secondary antibodies are indicated in Materials and methods. The bar at the bottom right represents 10 μm length. Manuscript in preparation.

4.4. **Objective 4.** To study TCR dynamics in such T-cell lines

4.4.1. TCR components of CD247-deficient T-cell lines

To unravel the components of the TCR due to the lack of CD247 deficiency, we immunoblotted whole-cell lysate (Lysate), increased amount of the lysate for the deficient cell lines (enriched whole-cell lysate or E. Lysate) or the immunoprecipitation product of the lysates with magnetics Protein G Dynabeads (IP) with anti-CD3εδ/εγ antibody (UCHT-1 clone). The enriched amount of E. Lysate or IP was proportional to the defect detected by each TCR antibody by intracellular flow cytometry (see Fig 3.2), except for TCRα or TCRβ for which an estimation of 20% of defect was assumed.

Regarding the partial CD247 deficiency, all TCR chains were detected in the IP conforming that octameric complex was assembled, like in the control cell line, but both TCRα and TCRβ showed different molecular weight compared to control (Fig 4.1). For the deficient cell line, CD247$^{-/-}$, both CD3δ, CD3γ and TCRα were immunoprecipitated but there was not detection of TCRβ.

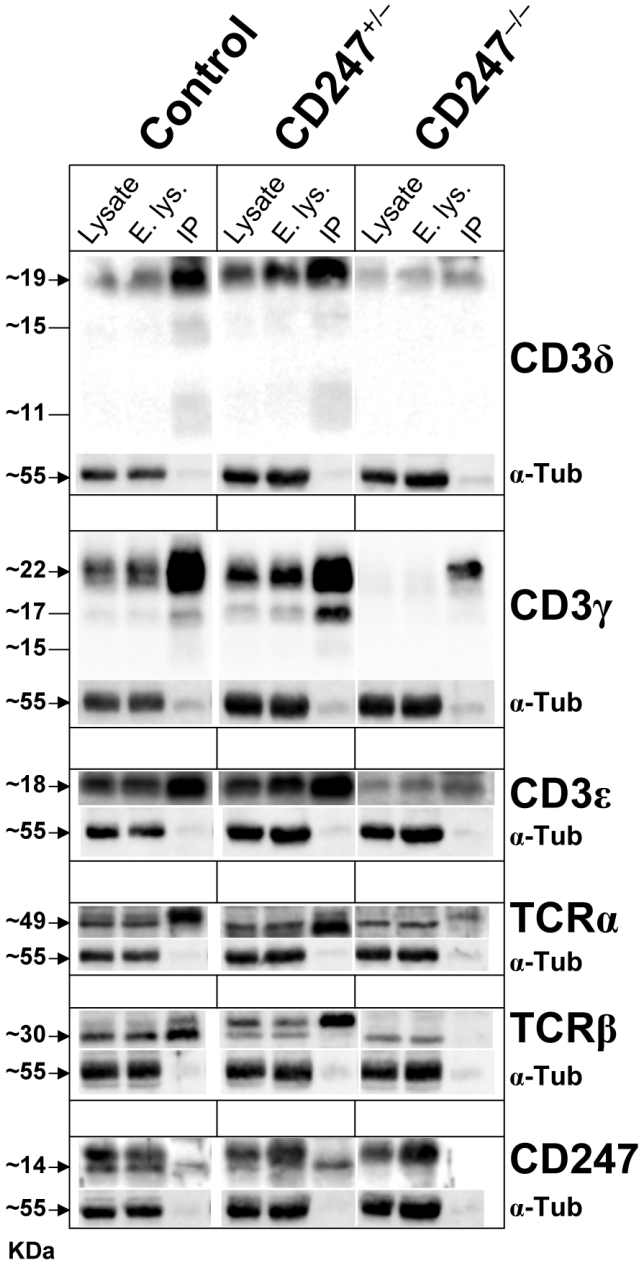

Figure 4.1. TCR components in one control, the patient revertant haploinsufficient or the CD247-deficient cell lines (CD247$^{+/-}$or CD247$^{-/-}$, respectively). Immunoprecipitation of minimal TCR subunits, CD3εδ/εγ, was performed by using UCHT-1 clone, followed by immunoblotting using mouse antibodies against CD3δ, CD3γ CD3ε, TCRα, TCRβ and CD247 (EP4426, EPR4517, EPR5361(2), H-142, H-197 and 448 clones, respectively) in combination with rabbit antibody against α-Tubulin. Secondary antibodies are indicated in Materials and methods. For each cell line and immunoblotting, 80 µg of whole-cell lysate (*Lysate*), slightly increase amount of whole-cell lysate (80-140 µg, enriched whole-cell lysate or *E. lys*) and IP product resulting from 1-2 mg of whole-cell lysate (IP) were used. Arrow in the left side of the figures indicates estimated molecular weight of every protein with the antibodies used. Data are representative of two independent experiments.

4.4.2. TCR trafficking and down-modulation after triggering

Regular TCR trafficking between cell surface and recycling compartment is a physiological pathway of TCR complex (Compeer *et al.*, 2018). To evaluate the functioning of the TCR recycling cycle in our cell lines, cells were treated with a reversible inhibitor of the anterograde pathway protein transportation (brefeldin A or BFA). In the first 60 minutes, a reduction of around 20% of original CD3 surface levels was detected in all cell lines (Fig 4.2). The control cell line recovered normal surface CD3 levels after 180 minutes of the treatment meanwhile CD247$^{+/-}$ did it at 400 minutes and the CD247$^{-/-}$ cell line never recovered its original surface CD3 levels (Fig 4.2), suggesting that CD247 was necessary to the operation of TCR-recycling cycle.

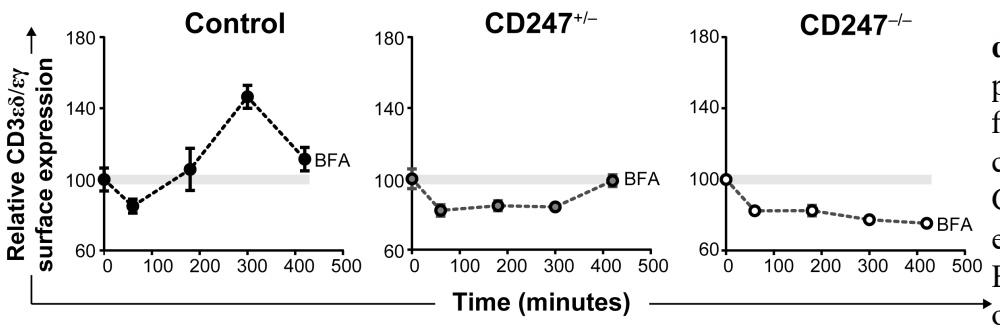

Figure 4.2. TCR surface dynamics in one control, the patient revertant haploinsufficient or the CD247-deficient cell lines (CD247$^{+/-}$ or CD247$^{-/-}$, respectively). The effect of brefeldin A (5 µg/mL, BFA) on the surface expression of CD3εδ/εγ (UCHT-1 clone) was determined by flow cytometry at the time points indicated. The relative CD3εδ/εγ surface expression (based on Geo-MFI values) is expressed as a percentage of the total surface levels in DMSO condition. These results correspond with data accumulated of 6 different experiments.

Another important mechanism of TCR regulation on the cell surface is the TCR internalization or down-modulated after engagement, that has been historically evaluated *in vitro* using agonist antibodies against CD3 chains. Then, cells were stimulated with an anti-CD3εδ/εγ antibody, the OKT-3 clone, until the indicated time points and the remaining CD3 on surface was measured by extracellular flow cytometry. The control cell line was able to down-modulate the CD3 until 10% of the original levels, being the half amount of surface CD3 or half-life was 12 minutes and the rate constant of surface expression decay (K, min^{-1}) of 0,058 min^{-1} (Fig 4.3, A and B). The performance and parameter values for the CD247$^{+/-}$ cell line were the same than the obtained for the control, suggesting that even though there was less amount of CD3 on cell surface it was absolutely functional (Fig 4.3, A and B). Regarding the CD247$^{-/-}$ cell line, it was only able to down-modulate the surface CD3 until around 35% of its original value, presenting a half-life of 9,51 minutes and a K of 0,072 min^{-1}, indicating that it took less time to internalize the half of the CD3 of the surface but the speed seemed lower than the control cell line (Fig 4.3, A and B). To determine if the results of the CD247$^{-/-}$ cell line were real or a technical artefact due to dramatically reduced surface CD3 levels, a similar assay was performed to evaluate the CD3 down-modulation but incubating the cells with lysosome inhibitor to avoid degradation after internalization, permeabilizing the cells to detect the total amount of protein and revealing by confocal microscopy to see the distribution within the cell. After CD3 stimulation, the signal that was detected in the periphery of the cell without stimulation was observed in remarkable spots inside the cell in both the control and CD247$^{-/-}$ cell lines (Fig 4.3, C), what corresponded with lysosome or early endosome compartments (data not included), confirming that the CD3 present in the cell surface in the CD247$^{-/-}$ cell line was actively down-modulated.

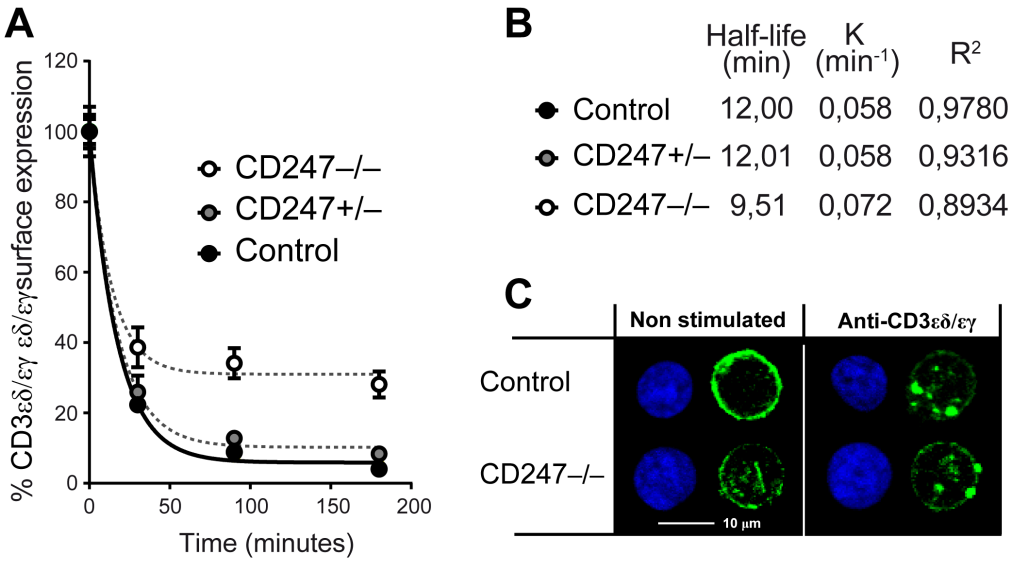

Figure 4.3. TCR down-modulation after CD3 triggering in one control, the patient revertant haploinsufficient or the CD247-deficient cell lines ($CD247^{+/-}$ or $CD247^{-/-}$, respectively). **A**, % CD3εδ/εγ surface expression (based on Geo-MFI values), relativized to absence of agonist antibody, for each T-cell line during time after anti-CD3εδ/εγ antibody stimulation (OKT-3 clone, 1 µg/mL) using goat anti-mouse PE as secondary antibody. **B**, the half-life (min) and the rate constant of surface expression decay (K, min^{-1}), was estimated applying a one-phase decay exponential in GraphPad Prism, obtaining acceptable R-square (R^2) values. **C**, Confocal microscopy was performed in control and $CD247^{-/-}$ cell lines after stimulation with 1 µg/mL OKT-3 and 10 µg/mL Goat F(ab')2 Anti-Mouse IgG (H+L) in presence of 100 µM chloroquine for 180 min, using the secondary antibody and DAPI as indicated in Materials and Methods (this is a representative result of one of the experiments). These results correspond with data accumulated of 6 different experiments.

4.4.3. Incomplete TCR subcellular localization

To determine whether or not the incomplete TCR was able to reach the cell surface despite not having all the necessary pieces, we studied colocalization of the minimal TCR subunit, CD3εδ/εγ heterodimers, with subcellular components markers for T-cells by confocal microscopy, as indicated in Figure 4.4. The technique was previously validated with blood CD4 T-cells confirming that HTLV-1 cell lines behaved similar to blood T cells (data not included). At first sight, we observed that CD3εδ/εγ was located in an outer layer than endoplasmic reticulum (ER) in control cell line, as expected, but for the cell lines with reduced amount of CD247 the distribution was switched, being CD3εδ/εγ in an inner layer than endoplasmic reticulum (Fig 4.4, A). The same switched distribution was observed for CD3εδ/εγ *vs* Cis- and Trans-Golgi (GM130 and TGN46, (respectively) and early endosomes (EEA1) markers, suggesting an aberrant CD3εδ/εγ heterodimers transportation to the surface (Fig 4.4, A). In terms of quantification of the colocalization, we observed that CD3εδ/εγ signal showed significative higher colocalization in ER (Clx) for reduced or complete absence of CD247 (Fig 4.4, B). In contrast to previous studies (Dietrich *et al.*, 1999), CD3εδ/εγ heterodimers were not accumulated in Cis-Golgi compartment for any case, indeed we observed fewer colocalization than for control cell line, also in Trans-Golgi compartment. CD3εδ/εγ was neither accumulated in early endosome compartment, indeed we found fewer colocalization than for control cell line. In contrast to that and according to previous studies in mouse *in vitro* model MA5.8, we observed higher accumulation of CD3εδ/εγ in lysosome (LAMP-1) for $CD247^{+/-}$ or $CD247^{-/-}$ cell lines (Fig 4.4, B), but the bigger changes were identified near to cell surface. Just like CD3εδ/εγ heterodimers were accumulated in ER for all mutant cell lines, they showed much lower colocalization than control in recycling compartment (CD71), and the same pattern was found for cell surface marker (CD4) (Fig 4.4, B), indicating that the main problem was in reaching the surroundings of the plasma membrane.

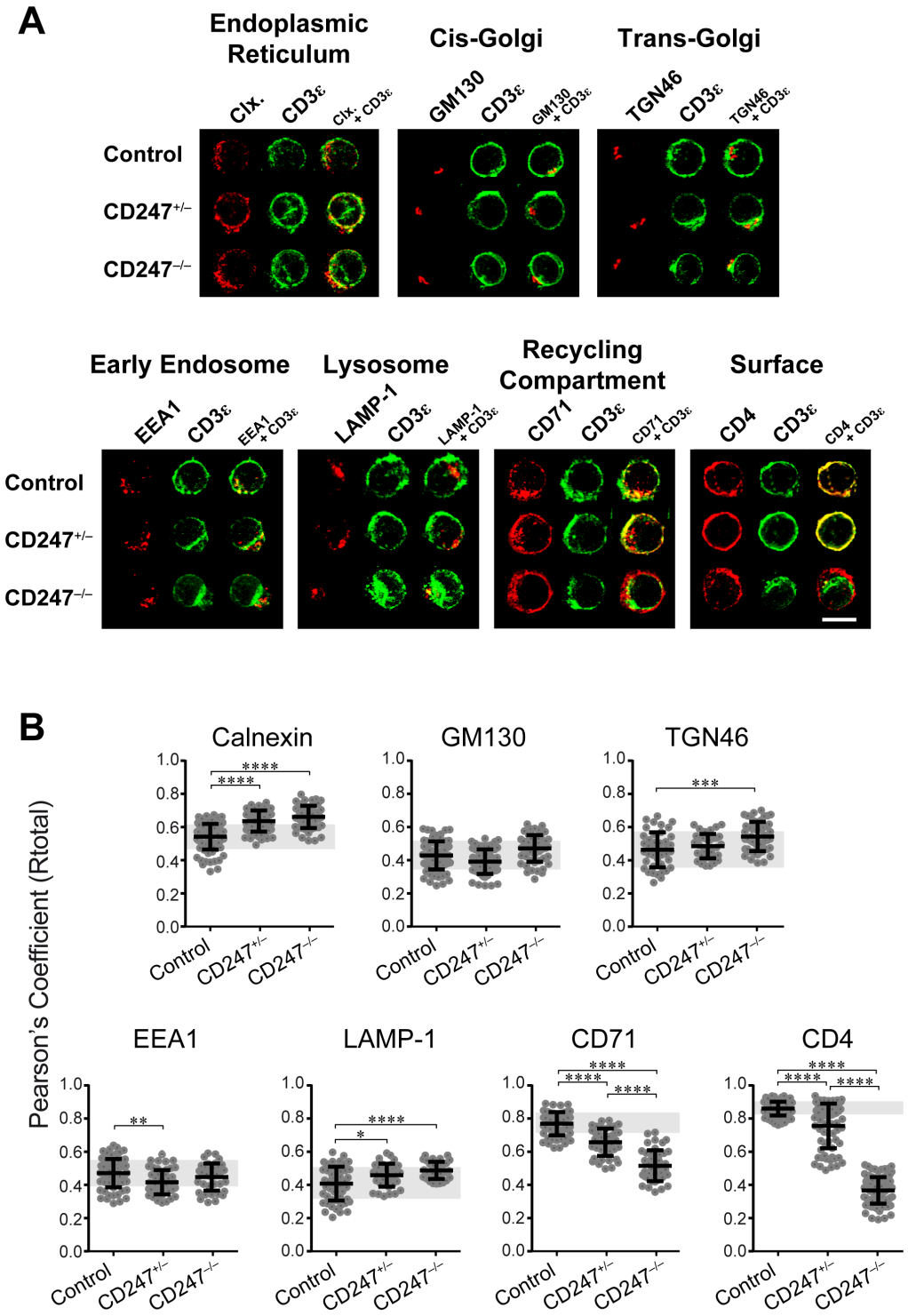

Figure 4.4. Subcellular CD3 localization in one control, the patient revertant haploinsufficient or the CD247-deficient cell lines (CD247$^{+/-}$ or CD247$^{-/-}$, respectively). **A**, confocal microscopy was performed in the indicated cell lines using antibodies against specific proteins of the endoplasmic reticulum (calnexin or Clx), cis-Golgi (GM130), trans-Golgi (TGN46), early endosome (early endosome antigen-1 or EEA2), lysosome (LAMP-1), recycling compartment (CD71) and cell surface (CD4) (all in red) in combination with anti- CD3εδ/εγ (UCHT-1 clone, green) and DAPI. Secondary antibodies are indicated in Materials and Methods. The bar at the bottom right represents 10 μm length. **B**, Pearson correlation coefficients Rcoloc from Fiji/ImageJ were used for statistical analysis for each subcellular marker in each cell line. Up to 100 different measurements accumulated from different experiments were considered for each subcellular marker. Statistical significance was assessed using 1-way ANOVA with Bonferroni multiple comparison (*P <0.05, **P < 0.01, ***P < 0.001, ****P < 0.0001).

4.4.4. TCR degradation pathway

Once we observed that some TCR chains showed reduced expression side by side of diminished or complete absence levels of CD247, we wonder if it was a consequence of a protein degradation process in term to maintain balanced amount of TCR chains. To unravel if any of the previously described mechanisms was relevant, lysosome- or endoplasmic reticulum-dependent proteasome degradation, first cells were cultured for 3 hours with chloroquine or MG132, inhibitors of lysosome or proteasome activity respectively, and extracellular CD3εδ/εγ and TCRαβ levels were measured by flow cytometry. In the control cell line, an increase of both surface CD3εδ/εγ and TCRαβ signal was observed with the proteasome inhibitor but no differences with the lysosome inhibitor (Fig 4.5), conferring to the ER-dependent proteasome degradation an active role in maintaining the amount of any of the TCR components or some regulators necessary to the synthesis in homeostasis. In the reduced amount of CD247 settings, using the CD247$^{+/-}$ cell line, any increase was observed with the proteasome but a significant decrease was detected with the lysosome inhibitor (Fig 4.5). In the CD247$^{-/-}$ cell line we could detect an increase of surface CD3εδ/εγ but not of TCRαβ signal after proteasome inhibitor treatment (Fig 4.5), suggesting that the complete absence of CD247 totally block the hexameric TCR assembly (TCRαβCD3εδ/εγ) but not the assembly and surface exportation of CD3εδ/εγ heterodimers without the variable heterodimer TCRαβ.

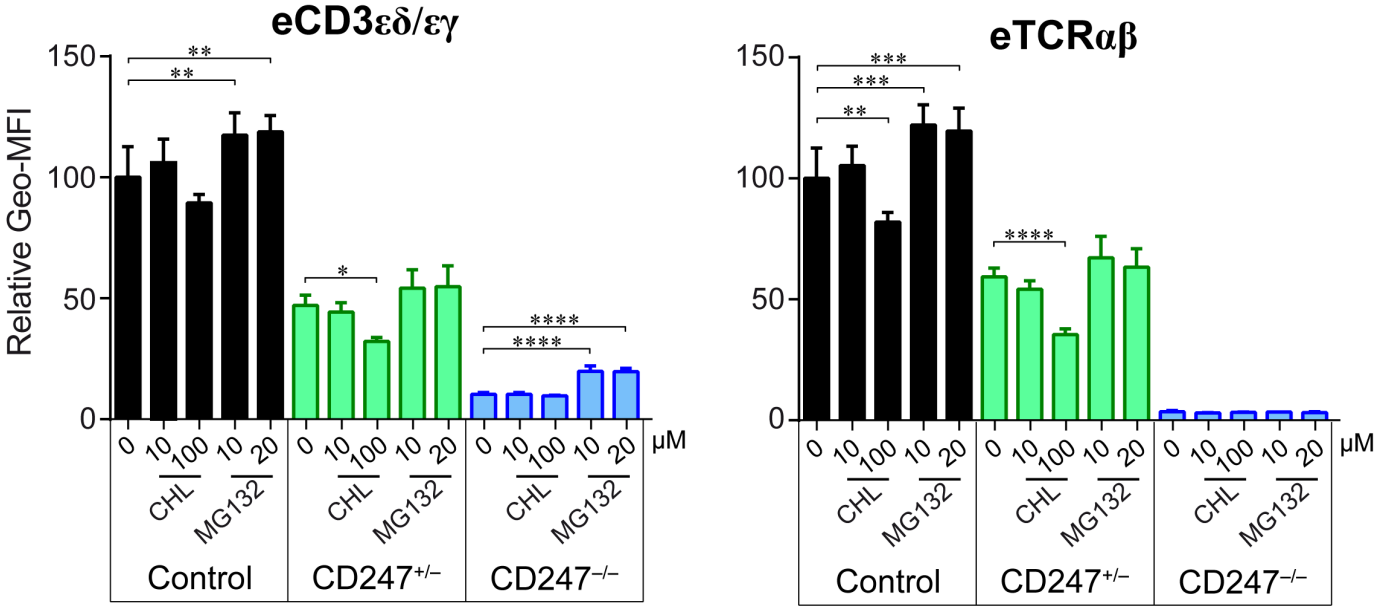

Figure 4.5. TCR degradation by flow cytometry studied in one control, the patient revertant haploinsufficient or the CD247-deficient cell lines (CD247$^{+/-}$ or CD247$^{-/-}$, respectively). T-cell lines were cultured for 180 minutes in the presence of DMSO as control, and chloroquine (10 or 100 μM) or MG132 (10 or 20 μM) to inhibit lysosome of proteasome activity, respectively, and surface levels (e, extracellular) of CD3εδ/εγ and TCRαβ (UCHT-1 and IP26 clones, respectively) were measured by flow cytometry. The *Relative Geo-MFI* is expressed as a percentage of the total surface levels relative to DMSO condition of control cell line. These results correspond with data accumulated of 9 different experiments. Statistical significance was assessed using 1-way ANOVA with Bonferroni multiple comparison (*P <0.05, **P < 0.01, ***P < 0.001, ****P < 0.0001).

To understand what relevant TCR chain would be degraded by ER-dependent proteasome pathway and then indirectly control the amount exported to the cell surface, the same procedure of lysosome or proteasome inhibition was performed but TCR chains were revealed by western blot. In all cell lines and independently of CD247 levels, we could detect additional signals of smaller molecular weight fragments of CD3δ and CD3γ (around 15 KDa), confirming that CD3δ is a target of proteasome degradation and adding CD3γ to the list (Fig 4.6). Unfortunately, we did not detect smaller bands of TCRα of CD247 as we expected because they contain sequences associated to proteasome degradation. Surprisingly, a mild CD247 band with wild type molecular weight was detected in the CD247$^{-/-}$ cell line after proteasome inhibition treatment.

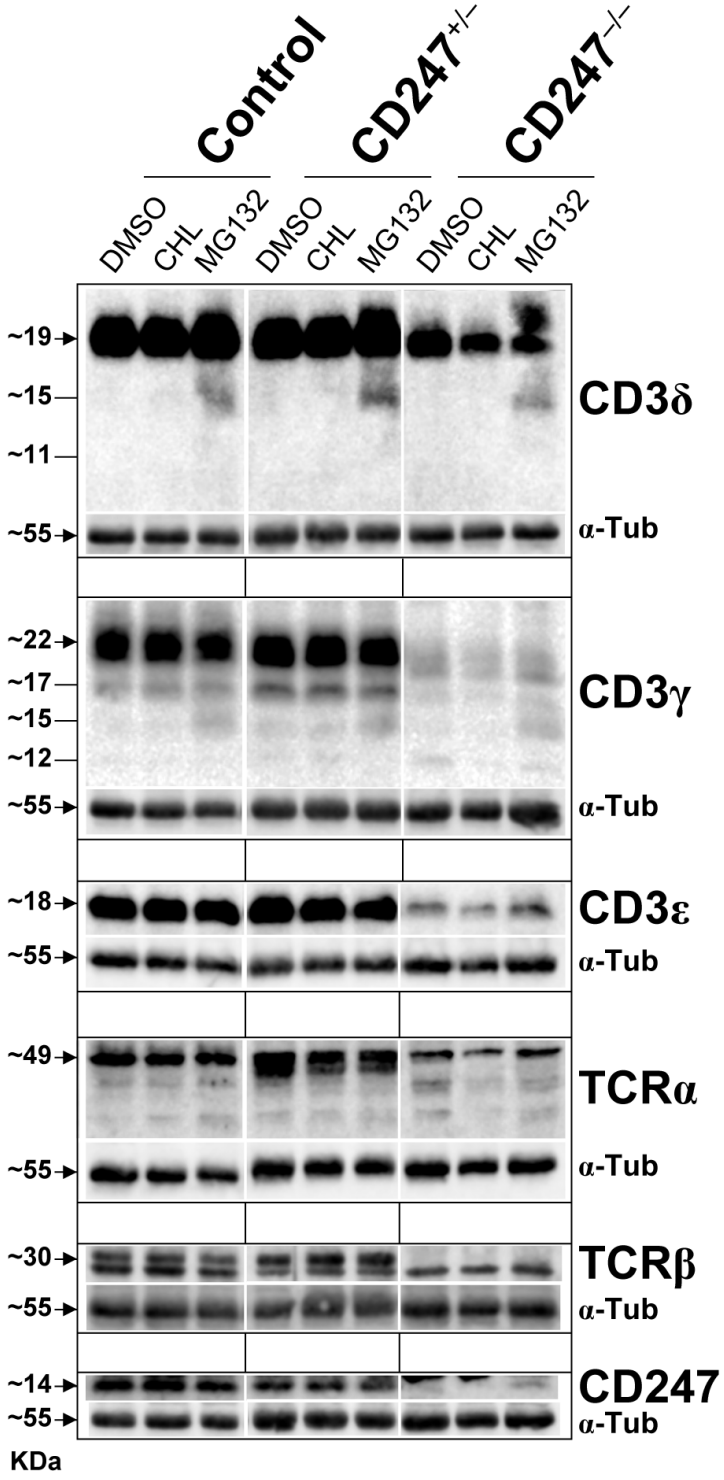

Figure 4.6. TCR degradation by western studied in one control, the patient revertant haploinsufficient or the CD247-deficient cell lines (CD247$^{+/-}$ or CD247$^{-/-}$, respectively). Cells were cultured in presence of DMSO, 100 µM chloroquine (CHL) or 10 µM MG132 for 3 hours and resulting whole-cell lysates were immunoblotted using the antibodies indicated in Figure 4.1. For each cell line and immunoblotting, 80-140 µg of whole-cell lysate were used. Arrow in the left side of the figures indicates estimated molecular weight of every protein with the antibodies used. Data are representative of two independent experiments.

5. DISCUSSION

The third CD247-deficient patient establishes the phenotype and severity of the pathology

In the first part of this work, we characterized the T-cell phenotype of a Turkish child carrying a homozygous c.2T>C mutation in CD247 that prevented translation by disrupting the initiation codon, thus causing complete CD247 deficiency (Fig 1.1 and 1.3). Although T-cell counts were not dramatically reduced in the patient, TCR surface levels were extremely low and corresponded with mendelian inheritance (Fig 1.2). We were able to expand patient CD247-deficient T-cells in vitro that were necessary for further studies (Fig 1.4). The T-cell development was clearly affected, as shown by the reduced variability of the TCRVβ repertoire and cell distribution (Fig 1.5 and Table 1.1). These data suggested that, as observed in mice (Love *et al.*, 1993; Sussman *et al.*, 1988), CD247 plays a critical role for T-cell selection in the thymus, yet partial TCR complexes lacking CD247 can signal to some extent for selection. It was interesting to observe that even though the T-cell development must be totally impaired without CD247, the CD247-deficient cells presented oligoclonal repertoire (Fig 1.5). CD247 participates in the assembly and surface expression of the TCR complex and in the delivery of intracellular signals, but its absence does not preclude membrane expression. Indeed, both human and mouse T-cells lacking CD247 have reduced but not ablated surface TCR expression (Rieux-Laucat *et al.*, 2006; Roberts *et al.*, 2007; Sussman *et al.*, 1988; Vales-Gomez *et al.*, 2016). Thus, we detected surface CD3 expression in the patient's T-cells, although forty-fold reduced compared to healthy individuals. Interestingly, surface CD3 expression in mutation carriers in *CD247*, but not for other TCR invariant chain genes, was reduced around two-fold (Fig 1.2), supporting that CD247 is rate-limiting for TCR assembly (Sussman *et al.*, 1988). Of note, the patient's T cells were mostly $CD8^+$, suggesting (i) a differential requirement of CD247 for thymic selection (Love *et al.*, 2000; Watanabe *et al.*, 2000) of $CD4^+$ versus $CD8^+$ lineage cells, or (ii) a selective expansion of the CD8+ subset in the periphery, perhaps related to chronic CMV infection (Gamadia *et al.*, 2001; Huygens *et al.*, 2014; Trimble *et al.*, 2000) or both. The selective $CD4^+$ T-cell lymphopenia observed in our patient fits with an inverted CD4/CD8 ratio in all three CD247-deficient patients (Table 1.2), and is in sharp contrast with the phenotype observed in zeta-associated protein (ZAP) 70-deficient patients, which show selective absence of mature $CD8^+$ T cells in the periphery (Turul *et al.*, 2009). These findings suggest that CD247 may interact with signalling molecules other than ZAP70 (Pacini *et al.*, 2000), and conversely, that ZAP70 may signal from receptors other than the TCR (Kumar *et al.*, 2006). The balance was that partial TCR complexes lacking CD247 can signal to some extent for selection because patient T-cells were able to proliferate upon the allogeneic condition (Fig 1.4), but the TCR without any CD247 was unable to induce activation markers, proliferation or phosphorylation in the canonical TCR pathway (Fig 1.6). Then the fact that CD247-deficient patients present mild lymphopenia should not confound the fact that CD247 deficiency, besides the totally impaired TCR signaling, is a very severe condition that requires urgent transplantation.

Patient revertant T-cells were functional, in contrast to previous cases

Regarding the revertant T-cells, this new patient resembled that of two other reported cases (Table 1.2 and Fig 1.7). In both, $CD3\varepsilon^{low}$ and $CD3\varepsilon^{high}$ T-cells were also identified and, in our patient, revertant T-cells presented TCR expression levels like carriers' as the reversion only occurred in one of the alleles. Given the low frequency of revertant T cells in vivo, it seems improbable that a single cell would carry both somatic mutations. In the first patient reported (Rieux-Laucat *et al.*, 2006), the

germinal mutation was located in the region that codified the first ITAM motif and 3 different somatic mutations (second-site) were reported, for which the software prediction indicated just an aminoacid change but the TCR signalling in these cells continued impaired. No molecular analysis for somatic mutations was reported for the second patient although they can be guessed by the phenotype (Roberts *et al.*, 2007). TCR signalling in our patient revertant T-cells were recovered to heterozygous levels (Fig 1.6) and were thus proportional to CD247 expression (Fig 1.3). The origin in terms of ontogeny of these revertant cells was not addressed in our study but the fact that TCRCβ1^{+} and TCRCβ1^{-} cells were identified (Fig 1.5) suggesting that it must be at least prior TCRβ gene rearrangement at the DN stage in T-cell development (Dudley *et al.*, 1994). Nevertheless, revertant T-cells in the patient were so scarce that clinical improvement did not occur and HSCT was finally carried out. So far, CD247 deficiency is the only TCRID in which T-cells carrying somatic mutations completely or partially reversing the germ-line mutation have been identified. Thus, the presence of revertants together with strongly reduced surface TCR expression are pathognomonic of CD247 deficiency (Garcillan *et al.*, 2015; A. V. M. Marin *et al.*, 2015).

In summary of the first objective of the research, our description of the third case of primary CD247 deficiency confirmed that the complete lack of CD247 causes SCID. Moreover, it clearly established that, in contrast to primary ID affecting other TCR chains, CD247-deficient T lymphocytes are prone to reversions. Our results showed that, despite being functional *in vitro*, revertant T-cells were scarce and unlikely to lead to significant recovery of adaptive immune functions *in vivo*, advising urgent HSCT even in the absence of severe lymphopenia.

Improved TCRID diagnostic procedure

In our work, we propose a new procedure to diagnose TCRID patients using PBMC samples by the combination of extracellular and intracellular flow cytometry stainings. We tested a substantial number of individuals from the same family of the CD247-deficient patient, samples that were received after two-days travelling in non-optimal conditions. We could sort out wild type, carriers or homozygous of the mutation of the family just by extracellular CD3 flow cytometry and determine the precise cause of the defect identifying a complete absence of CD247 in the patient by intracellular flow cytometry (Fig 2.1) using a procedure that can take up to 2 hours in contrast to genetic studies that can last several days. The carriers of other CD247 mutations of the reported patients were not studied (Rieux-Laucat *et al.*, 2006; Roberts *et al.*, 2007). Also, although up to 20% of surface CD3 reduction has been reported in T-cells of CD3γ or CD3δ haploinsufficiency donors (Munoz-Ruiz *et al.*, 2013), it was not associated to any diagnostic value. The procedure of patient TCRID diagnosis is based on clinical features and genetic findings, including the progenitors' study to determine patterns of inheritance (A. V. M. Marin *et al.*, 2015). Our approach, together but sooner that genetic studies, accelerates the diagnostic procedure necessary to proceed with the suitable therapy using simple and low-cost protocols and reagents.

In vitro T-cell models recapitulated peripheral blood T lymphocytes from the patient and mutation carriers

In the third and fourth objectives of this work, we characterized the biology of the TCR complex resultant from the complete or partial CD247-deficient cell lines derived from the reported patient and family members. Starting from the TCR phenotype, the *in vitro* generated T-cell lines from the

CD247-deficient patient, $CD247^{+/-}$ or $CD247^{-/-}$ for the revertant or germ line mutation cells respectively, totally resembled the original levels of surface and intracellular TCR/CD3 chains (Fig 3.1 and 3.2), indicating that the immortalization process with the HTLV-1 did not affected the genuineness of the cells. In the same line, the surface CD3 levels of carrier's primary or immortalized T-cells were comparable (Fig 3.1). Historically, only a murine cell line has been available to address the complete CD247 deficiency, the MA5.8 (Geisler *et al.*, 1989), in which surface CD3 levels also suffered a dramatic decrease due to the lack of CD247. Considering the requirements and steps of the correct assembly of the TCR and in contrast to previous data (Borroto *et al.*, 1998; Call & Wucherpfennig, 2005; Malissen *et al.*, 1999; Natarajan *et al.*, 2016), we observed that when CD247 was totally absence, the CD3εδ/εγ heterodimers were able to reach the cell surface even not associated to TCRα or TCRβ (Fig 3.1). It was surprising to observe that other TCR chains had diminished levels in our *in vitro* cell lines whenever CD247 was partially or complete absent (Fig 3.2), fact that was not previously reported for the MA5.8 cell line, suggesting that CD247 may have a regulatory role over the synthesis or stability of other TCR chains that do not find the correspondent pieces to form the receptor (Wileman *et al.*, 1990). It also leaded the debate about the usefulness of any gene therapy that would supply the lack of CD247 and if it would restore the normal levels of other TCR chains, what needs to be studied more deeply. Anyhow, these results were important to take into consideration because other pathologies debut with reduced CD247 levels like SLE (Martins *et al.*, 2015) or certain types of cancer (Christopoulos *et al.*, 2015), and that can affect levels of other TCR chains.

The hexameric TCR is not assembled in CD247-deficient T cells

In the MA5.8 murine *in vitro* model of CD247 deficiency, it was simultaneously demonstrated that the absence of CD247 allowed the formation of structures formed by αβγδε, αβδε and αβγε chains (Bonifacino *et al.*, 1988) and that the CD3γ/δ/ε chains were much less abundant on the cell surface that in normal condition (Sussman *et al.*, 1988). Alternatively, it was reported that incomplete TCR structures, in which first TCRα and TCRβ chains joined CD3 heterodimers independently, were formed in the ER, in this case using a human model, Jurkat cell lines (Alarcon *et al.*, 1988). All together supposed that the scientific community assumed the paradigm that the structure that reached the cell surface in absence of CD247 was an hexameric complex, αβγεδε (Dietrich *et al.*, 1999). In contrast, our results indicated that in complete absence of CD247, the CD3 heterodimers could be joined to TCRα but not to TCRβ (Fig 4.1), suggesting as the possible structures αγε and/or αδε, δε and γε, what was in the line of the Jurkat cell line results (Alarcon *et al.*, 1988). We could detect an increased amount of CD3 heterodimers after proteasome inhibition in the CD247-deficient cell line but the signal of the antibody against the conformational epitope TCRαβ was still negative (Fig 4.5) and it was never detected in patient T-cell using different clones (data not included). We could also observe that, in both partial or complete CD247-deficient cell lines, TCRα and TCRβ had different molecular weights than control although the diminished levels (Fig 4.1), a phenomena that was previously described for $CD3\gamma^{-/-}$ patient cell line (Zapata *et al.*, 2004), suggesting altered glycosylation levels of these proteins in the absence of CD247. Our evidence demonstrates that the paradigm of the hexameric TCR was not correct for human or at least the composition is not detectable, emphasizing the differences between human and mouse TCR.

Despite their scarcity, CD247-deficient TCR ensembles could be internalized using brefeldin-A or an anti-CD3εδ/εγ agonist antibody, but they were not reincorporated to the cell surface via recycling (Fig 4.2 and 4.3). The active TCR modulation measured after brefeldin-A treatment suggested that

the protein regions associated to internalization were maintained in human CD247 deficiency despite the crippled structure (Liu *et al.*, 2000), but not the ones that mediate cell surface reincorporation as observed in CD3γ deficiency (Torres *et al.*, 2003). Again, kinetics of TCR internalization are different between mouse and human in CD247 deficiency, since CD3 endocytosis was faster in the murine MA5.8 comparing to its wild-type cell line (2B4) and slower in our human CD247-deficient cell line comparing to its control, demonstrating that CD247 in the TCR structures has specific roles depending on the specie.(D'Oro *et al.*, 2002).

CD247 is incorporated in the ER, rather than Golgi apparatus in normal T cells

Using Jurkat cell clones with different mutations on TCR genes but not CD247, it was described that CD247 was transported to and retained in the Golgi apparatus independently of other TCR chains, because CD247 colocalized with a Golgi marker and not with a lysosome marker by confocal microcopy (Dietrich *et al.*, 1999). The authors also demonstrated that in the MA5.8 cell line the CD3 also colocalized with Golgi markers (Dietrich *et al.*, 1999), concluding that CD247 must be incorporated to a hexameric TCR in the Golgi apparatus. We tested the hypothesis studying colocalization of different subcellular compartments markers, including some additional to those previous reported, with CD3 in up to 100 measurements for each marker and cell line, observing increased levels of colocalization in ER but not in Golgi apparatus in CD247 deficiency (Fig 4.4), suggesting that then the incorporation of CD247 must be in the ER, in opposite to previous data. The disagreement between our and previous data may be related to the cell lines used, considering our models extremely similar to human model because they were originally generated from them, but also that our technical approach was able to include hundreds of measurements instead of two.

Endoplasmic reticulum-proteasome dependent pathway seemed to control surface TCR and intracellular CD3δ and CD3γ levels

About the TCR degradation processes, the lysosome or the ER-proteasome dependent pathways are the two alternatives reported (Bonifacino, Cosson*, et al.*, 1990; Briant *et al.*, 2015; Dietrich *et al.*, 1999; Sussman *et al.*, 1988; Tiwari & Weissman, 2001; Werner *et al.*, 1996; Yang *et al.*, 1998), considering the lysosome the much more accepted by the scientific community (Dietrich *et al.*, 1999). Given that most of the previous studies were performed in mouse cell lines and encompassed just a single image of confocal microscopy, we wanted to understand what was the main TCR chains degradation mechanism in human. In the first approach by incubating the cells with lysosome or proteasome inhibitors and detecting the surface CD3 or TCRαβ by extracellular flow cytometry after, we could identify relevance of the ER-proteasome dependent pathway in the control cell line or in TCR chains homeostasis (Fig 4.5). A different result was the observed in the CD247-deficient cell line, for which also the ER-proteasome but not the lysosome dependent pathway was relevant and also revealed that only the CD3 heterodimers were increased in the cell surface. Then we expected to observe increased amounts of certain TCR chains after proteasome inhibition, and we could confirm by western blot that CD3δ, but not TCRα, was susceptible to degradation via proteasome, observing a small band after incubating the cells with the proteasome inhibitor (Fig 4.6), in all studied cell lines. We also could detect several smaller than normal weight bands correspondent to CD3γ, suggesting that this TCR chain is also susceptible to proteasome mechanism even though no proteasome degradation sequence has been reported in the literature (Bonifacino *et al.*, 1991; Carrasco *et al.*, 2001; Delgado & Alarcon, 2005; Mallabiabarrena *et al.*, 1992). Our results supporting the ER-proteasome dependent pathway as

the more relevant mechanism to control TCR chains levels and/or surface exportation and considering that there is no direct evidence but conjecture in the literature of the participation of the lysosome in the TCR homeostasis, we concluded that at least in human the preferent TCR chains degradation mechanism was the ER-proteasome dependent pathway.

In summary of the study of the generated cell lines, we have stablished new *in vitro* models of TCRID that resemble the real and severe situation of the patients and improve the actual models based on mouse or Jurkat cell lines, but also support new basis refining known processed as the incorporation of CD247 to the hexameric TCR in the ER instead of the Golgi apparatus (Fig Summary 1). We described the real severity of the CD247 deficiencies showing how all TCR chains may be affected in terms of amount or location when other TCR component is lacking and state that in human T-cells the main degradation mechanism of uncomplete TCR complex was the ER- proteasome dependent but not lysosome pathway (Fig Summary 2). These findings and *in vitro* models themselves should be taken into consideration for the development of new therapies for diseases such as malignancies of T-cells by targeting the TCR as is now being studied for leukemia (Dos Santos *et al.*, 2019) but also to comprehend new trendy aspects of T-cells such as endocytic TCR signaling for which this models that selectively affect one TCR chain may be absolutely useful (Saveanu *et al.*, 2019).

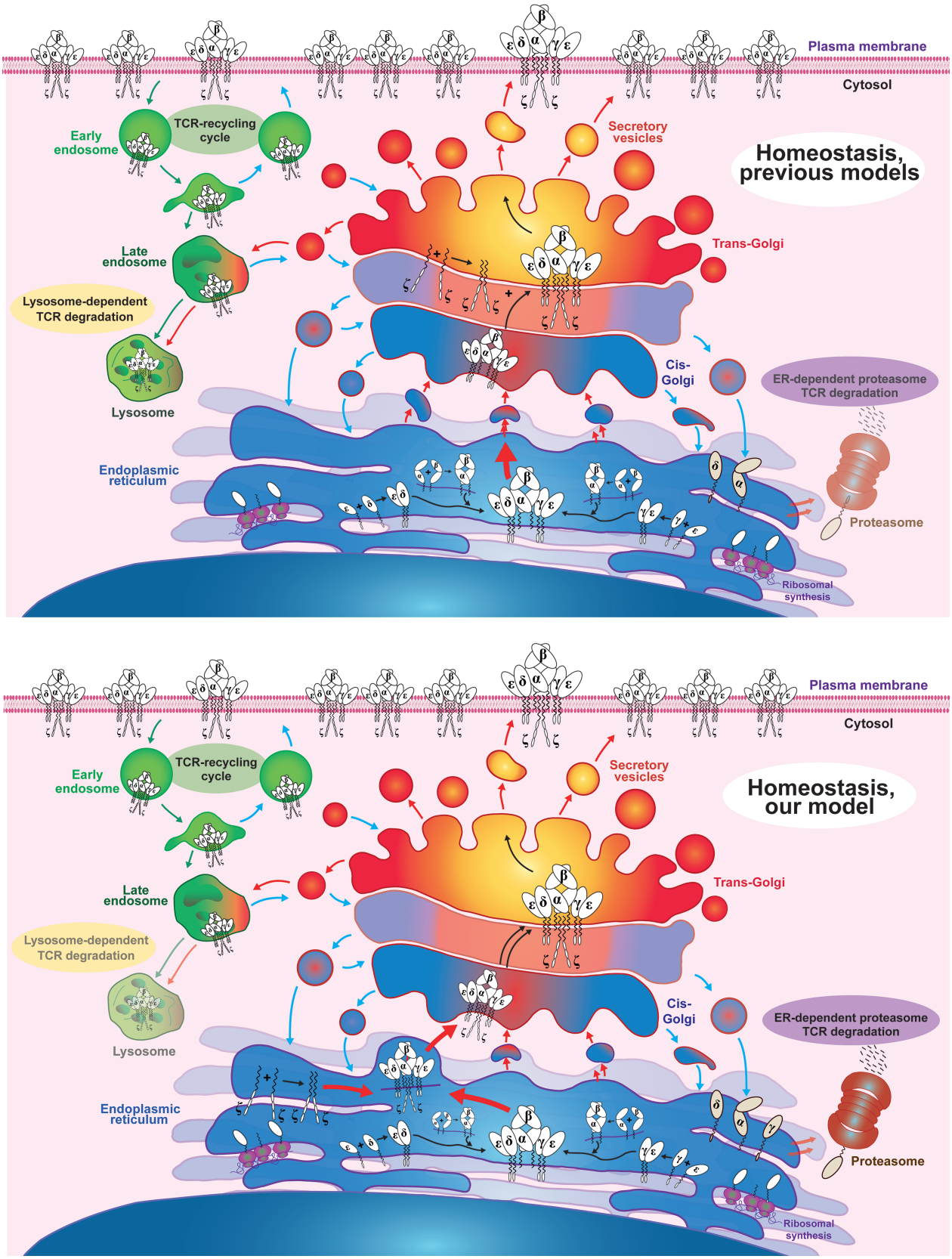

Figure Summary 1. Comparison of the TCR dynamics of data reported in the literature *vs* our results. The new data suggest that octameric TCR is assembled in the endoplasmic reticulum (ER) instead of Golgi apparatus and that the ER-dependent proteasome pathway has more relevance that the lysosome-dependent in contribution to TCR degradation.

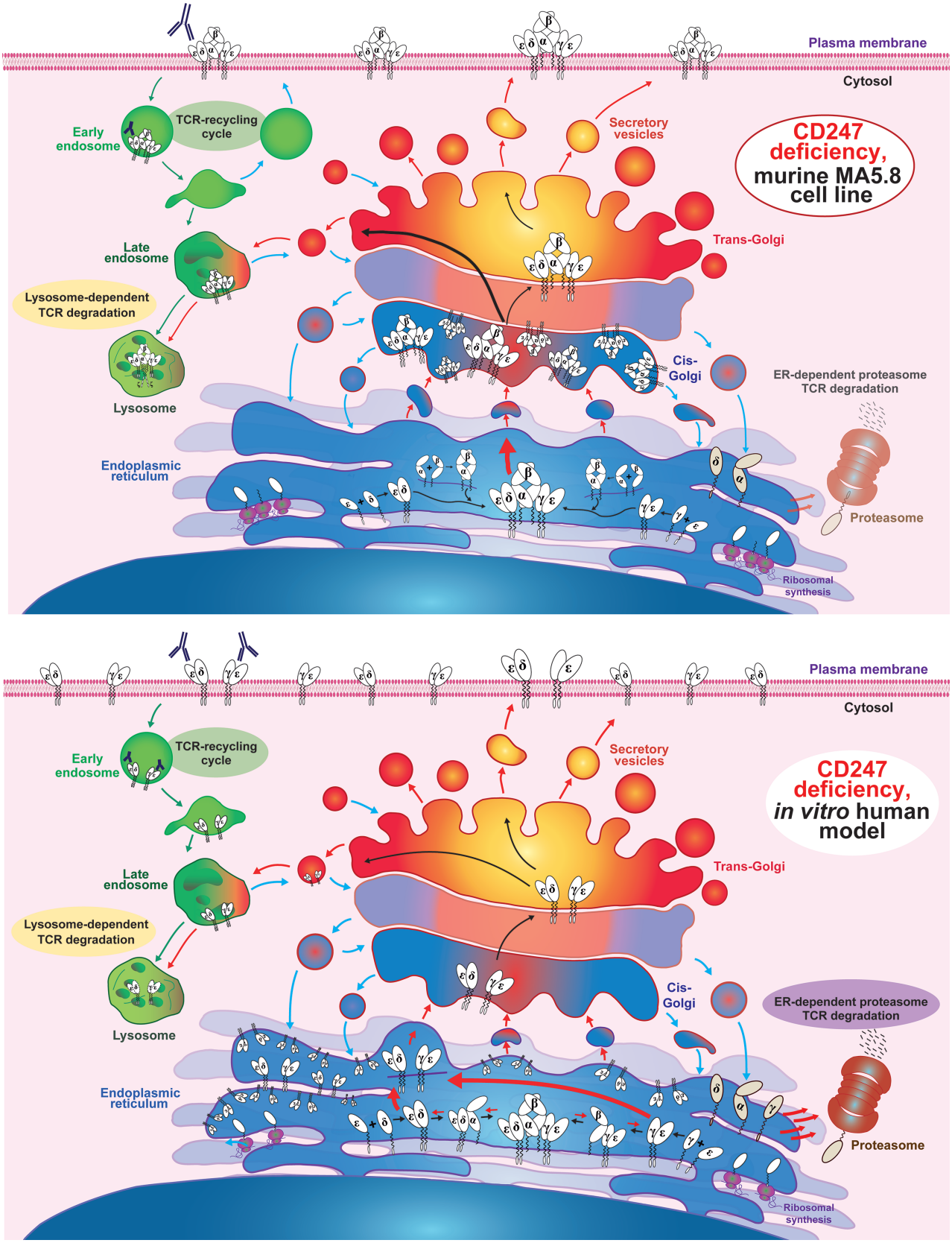

Figure Summary 2. Comparison of the TCR dynamics in the CD247-deficiency of data reported in the literature based on the murine MA5.8 *vs* our results in human HTLV-1 cell line. The new data suggest that (1) most TCR chains are forming heterodimers instead of an hexameric complex, (2) that are accumulated in the endoplasmic reticulum (ER) instead of the Golgi apparatus, (3) that the amount of the TCR chains that reach the cell surface are partially regulated by the ER- proteasome instead of lysosome-dependent degradation pathway, (4) that these TCR chains that reach the plasma membrane are CD3 heterodimers instead of an hexameric complex that lacks CD247, (5) and that these CD3 heterodimers can be translocated to the early endosomes after anti-CD3 triggering but unable to go back to the plasma membrane by the TCR recycling cycle.

6. CONCLUSIONS

Objective 1. To characterize a congenital CD247 ID

- We reported a new *CD247* mutation (c.2T>C) that codified for a truncated protein that was undetectable and caused a severe surface TCR expression and signaling defect.

- A small percentage of T cells recovered TCR expression and signaling levels of carriers due to two different somatic mutations, a second site mutation and a revertant.

Objective 2. To improve the diagnosis of TCRID

- We devised a fast (<4 h), simple and affordable intracellular flow cytometry protocol to diagnose TCRID in venous blood.

Objective 3. To generate patient-derived CD247-deficient and -haploinsufficient T-cell lines

- The T-cell lines recapitulated the phenotype of complete (—/—) or partial (+/—) CD247-deficient primary αβ T cells.

- The CD247 protein defect was together with decreased amounts of CD3δ, γ and ε chains, confirming the importance of the adequate balance of TCR proteins.

Objective 4. To study TCR dynamics in such T-cell lines

- The immunoprecipitation assays showed that CD3 εγ and εδ heterodimers were bound to TCRαβ in +/+ and +/— cells, but only to TCRα in —/— cells, weakening the existence of a hexameric αβεγεδ TCR before CD247 assembly.

- Engaged surface CD247-negative TCR could to be internalized but not recycled.

- The confocal microscopy studies indicated that CD3 chains accumulated in the ER rather than in the Golgi apparatus in —/— cells, suggesting that CD247 is incorporated to the TCR in the ER in normal T cells, as confirmed in +/+ and +/— cells.

- Inhibition experiments indicated that surface TCR increased in both CD247-deficient and –sufficient T cells when the proteasome, but not the lysosome, was blocked, supporting a proteasome- rather than lysosome-dependent TCR degradation pathway.

7. REFERENCES

Aksu, G., et al. (2006). Serum immunoglobulin (IgG, IgM, IgA) and IgG subclass concentrations in healthy children: a study using nephelometric technique. Turk J Pediatr, 48(1), 19-24.

Alarcon, B., et al. (1988). Assembly of the human T cell receptor-CD3 complex takes place in the endoplasmic reticulum and involves intermediary complexes between the CD3-gamma.delta.epsilon core and single T cell receptor alpha or beta chains. J Biol Chem, 263(6), 2953-2961.

Alcover, A., et al. (2018). Cell Biology of T Cell Receptor Expression and Regulation. Annu Rev Immunol, 36, 103-125. doi:10.1146/annurev-immunol-042617-053429

Arnaiz-Villena, A., et al. (1992). Brief report: primary immunodeficiency caused by mutations in the gene encoding the CD3-gamma subunit of the T-lymphocyte receptor. N Engl J Med, 327(8), 529-533. doi:10.1056/nejm199208203270805

Arnett, K. L., et al. (2004). Crystal structure of a human CD3-epsilon/delta dimer in complex with a UCHT1 single-chain antibody fragment. Proc Natl Acad Sci U S A, 101(46), 16268-16273. doi:10.1073/pnas.0407359101

Bonifacino, J. S., et al. (1988). Subunit interactions within the T-cell antigen receptor: clues from the study of partial complexes. Proc Natl Acad Sci U S A, 85(18), 6929-6933. doi:10.1073/pnas.85.18.6929

Bonifacino, J. S., et al. (1990). Colocalized transmembrane determinants for ER degradation and subunit assembly explain the intracellular fate of TCR chains. Cell, 63(3), 503-513. doi:10.1016/0092-8674(90)90447-m

Bonifacino, J. S., et al. (1991). Role of potentially charged transmembrane residues in targeting proteins for retention and degradation within the endoplasmic reticulum. Embo j, 10(10), 2783-2793.

Bonifacino, J. S., et al. (1990). A peptide sequence confers retention and rapid degradation in the endoplasmic reticulum. Science, 247(4938), 79-82. doi:10.1126/science.2294595

Bonifacino, J. S., et al. (1989). Pre-Golgi degradation of newly synthesized T-cell antigen receptor chains: intrinsic sensitivity and the role of subunit assembly. J Cell Biol, 109(1), 73-83. doi:10.1083/jcb.109.1.73

Borroto, A., et al. (1998). Characterization of the region involved in CD3 pairwise interactions within the T cell receptor complex. J Biol Chem, 273(21), 12807-12816. doi:10.1074/jbc.273.21.12807

Briant, K., et al. (2015). ERAD of proteins containing aberrant transmembrane domains requires ubiquitylation of cytoplasmic lysine residues. J Cell Sci, 128(22), 4112-4125. doi:10.1242/jcs.171215

Call, M. E., et al. (2002). The organizing principle in the formation of the T cell receptor-CD3 complex. Cell, 111(7), 967-979. doi:10.1016/s0092-8674(02)01194-7

Call, M. E., et al. (2004). Stoichiometry of the T-cell receptor-CD3 complex and key intermediates assembled in the endoplasmic reticulum. Embo j, 23(12), 2348-2357. doi:10.1038/sj.emboj.7600245

Call, M. E., et al. (2005). The T cell receptor: critical role of the membrane environment in receptor assembly and function. Annu Rev Immunol, 23, 101-125. doi:10.1146/annurev.immunol.23.021704.115625

Campbell, I. M., et al. (2015). Somatic mosaicism: implications for disease and transmission genetics. Trends Genet, 31(7), 382-392. doi:10.1016/j.tig.2015.03.013

Carrasco, Y. R., et al. (2001). An endoplasmic reticulum retention function for the cytoplasmic tail of the human pre-T cell receptor (TCR) alpha chain: potential role in the regulation of cell surface pre-TCR expression levels. J Exp Med, 193(9), 1045-1058. doi:10.1084/jem.193.9.1045

Castagnoli, R., et al. (2019). Hematopoietic Stem Cell Transplantation in Primary Immunodeficiency Diseases: Current Status and Future Perspectives. Front Pediatr, 7, 295. doi:10.3389/fped.2019.00295

Christopoulos, P., et al. (2015). A novel thymoma-associated immunodeficiency with increased naive T cells and reduced CD247 expression. J Immunol, 194(7), 3045-3053. doi:10.4049/jimmunol.1402805

Compeer, E. B., et al. (2018). A mobile endocytic network connects clathrin-independent receptor endocytosis to recycling and promotes T cell activation. Nat Commun, 9(1), 1597. doi:10.1038/s41467-018-04088-w

D'Oro, U., et al. (2002). Regulation of constitutive TCR internalization by the zeta-chain. J Immunol, 169(11), 6269-6278. doi:10.4049/jimmunol.169.11.6269

Dadi, H. K., et al. (2003). Effect of CD3delta deficiency on maturation of alpha/beta and gamma/delta T-cell lineages in severe combined immunodeficiency. N Engl J Med, 349(19), 1821-1828. doi:10.1056/NEJMoa031178

Davis, B. R., et al. (2009). Revertant somatic mosaicism in the Wiskott-Aldrich syndrome. Immunol Res, 44(1-3), 127-131. doi:10.1007/s12026-008-8091-4

Delgado, P., et al. (2005). An orderly inactivation of intracellular retention signals controls surface expression of the T cell antigen receptor. J Exp Med, 201(4), 555-566. doi:10.1084/jem.20041133

Dietrich, J., et al. (1994). CD3 gamma contains a phosphoserine-dependent di-leucine motif involved in down-regulation of the T cell receptor. Embo j, 13(9), 2156-2166.

Dietrich, J., et al. (1999). TCRzeta is transported to and retained in the Golgi apparatus independently of other TCR chains: implications for TCR assembly. Eur J Immunol, 29(5), 1719-1728. doi:10.1002/(SICI)1521-4141(199905)29:05<1719::AID-IMMU1719>3.0.CO;2-M

Dong, et al. (2019). Structural basis of assembly of the human T cell receptor-CD3 complex. Nature, 573(7775), 546-552. doi:10.1038/s41586-019-1537-0

Dos Santos, N. R., et al. (2019). The TCR/CD3 complex in leukemogenesis and as a therapeutic target in T-cell acute lymphoblastic leukemia. Adv Biol Regul, 74, 100638. doi:10.1016/j.jbior.2019.100638

Dudley, E. C., et al. (1994). T cell receptor beta chain gene rearrangement and selection during thymocyte development in adult mice. Immunity, 1(2), 83-93. doi:10.1016/1074-7613(94)90102-3

Firtina, S., et al. (2017). A novel pathogenic frameshift variant of CD3E gene in two T-B+ NK+ SCID patients from Turkey. Immunogenetics, 69(10), 653-659. doi:10.1007/s00251-017-1005-7

Gamadia, L. E., et al. (2001). Differentiation of cytomegalovirus-specific CD8(+) T cells in healthy and immunosuppressed virus carriers. Blood, 98(3), 754-761. doi:10.1182/blood.v98.3.754

Garcillan, B., et al. (2015). gammadelta T Lymphocytes in the Diagnosis of Human T Cell Receptor Immuno-

deficiencies. Front Immunol, 6, 20. doi:10.3389/fimmu.2015.00020

Geisler, C., et al. (1989). Failure to synthesize the human T-cell CD3-zeta chain and its consequence for the T-cell receptor-CD3 complex expression. Scand J Immunol, 30(2), 191-197. doi:10.1111/j.1365-3083.1989.tb01201.x

Gil, J., et al. (2011). A leaky mutation in CD3D differentially affects alphabeta and gammadelta T cells and leads to a Talphabeta-Tgammadelta+B+NK+ human SCID. J Clin Invest, 121(10), 3872-3876. doi:10.1172/JCI44254

Gokturk, B., et al. (2014). CD3G gene defects in familial autoimmune thyroiditis. Scand J Immunol, 80(5), 354-361. doi:10.1111/sji.12200

Huygens, A., et al. (2014). Immunity to cytomegalovirus in early life. Front Immunol, 5, 552. doi:10.3389/fimmu.2014.00552

Ikinciogullari, A., et al. (2004). Peripheral blood lymphocyte subsets in healthy Turkish children. Turk J Pediatr, 46(2), 125-130.

Kjer-Nielsen, L., et al. (2004). Crystal structure of the human T cell receptor CD3 epsilon gamma heterodimer complexed to the therapeutic mAb OKT3. Proc Natl Acad Sci U S A, 101(20), 7675-7680. doi:10.1073/pnas.0402295101

Kumar, A., et al. (2006). CXCR4 physically associates with the T cell receptor to signal in T cells. Immunity, 25(2), 213-224. doi:10.1016/j.immuni.2006.06.015

Liu, H., et al. (2000). On the dynamics of TCR:CD3 complex cell surface expression and downmodulation. Immunity, 13(5), 665-675. doi:10.1016/s1074-7613(00)00066-2

Love, P. E., et al. (2010). ITAM-mediated signaling by the T-cell antigen receptor. Cold Spring Harb Perspect Biol, 2(6), a002485. doi:10.1101/cshperspect.a002485

Love, P. E., et al. (2000). Critical relationship between TCR signaling potential and TCR affinity during thymocyte selection. J Immunol, 165(6), 3080-3087. doi:10.4049/jimmunol.165.6.3080

Love, P. E., et al. (1993). T cell development in mice that lack the zeta chain of the T cell antigen receptor complex. Science, 261(5123), 918-921. doi:10.1126/science.7688481

Malissen, B., et al. (1999). Function of the CD3 subunits of the pre-TCR and TCR complexes during T cell development. Adv Immunol, 72, 103-148. doi:10.1016/s0065-2776(08)60018-8

Mallabiabarrena, A., et al. (1992). An endoplasmic reticulum retention signal in the CD3 epsilon chain of the T-cell receptor. Nature, 357(6379), 593-596. doi:10.1038/357593a0

Marin, A. V., et al. (2017). Primary T-cell immunodeficiency with functional revertant somatic mosaicism in CD247. J Allergy Clin Immunol, 139(1), 347-349 e348. doi:10.1016/j.jaci.2016.06.020

Marin, A. V. M., et al. (2015). Human congenital T-cell receptor disorders. LymphoSign Journal, 2(1), 3-19. doi:10.14785/lpsn-2014-0012

Martinez-Martin, N., et al. (2011). T cell receptor internalization from the immunological synapse is mediated by TC21 and RhoG GTPase-dependent phagocytosis. Immunity, 35(2), 208-222. doi:10.1016/j.immu-

ni.2011.06.003

Martins, M., et al. (2015). Genetic association of CD247 (CD3zeta) with SLE in a large-scale multiethnic study. Genes Immun, 16(2), 142-150. doi:10.1038/gene.2014.73

Minami, Y., et al. (1987). Building a multichain receptor: synthesis, degradation, and assembly of the T-cell antigen receptor. Proc Natl Acad Sci U S A, 84(9), 2688-2692. doi:10.1073/pnas.84.9.2688

Moncada-Vélez, M., et al. (2011). Somatic mosaicism caused by monoallelic reversion of a mutation in T cells of a patient with ADA-SCID and the effects of enzyme replacement therapy on the revertant phenotype. Scand J Immunol, 74(5), 471-481. doi:10.1111/j.1365-3083.2011.02593.x

Monjas, A., et al. (2004). Engaged and bystander T cell receptors are down-modulated by different endocytotic pathways. J Biol Chem, 279(53), 55376-55384. doi:10.1074/jbc.M409342200

Morbach, H., et al. (2010). Reference values for B cell subpopulations from infancy to adulthood. Clin Exp Immunol, 162(2), 271-279. doi:10.1111/j.1365-2249.2010.04206.x

Morgan, N. V., et al. (2011). Mutation in the TCRalpha subunit constant gene (TRAC) leads to a human immunodeficiency disorder characterized by a lack of TCRalphabeta+ T cells. J Clin Invest, 121(2), 695-702. doi:10.1172/JCI41931

Munoz-Ruiz, M., et al. (2013). Human CD3gamma, but not CD3delta, haploinsufficiency differentially impairs gammadelta versus alphabeta surface TCR expression. BMC Immunol, 14, 3. doi:10.1186/1471-2172-14-3

Natarajan, A., et al. (2016). Structural Model of the Extracellular Assembly of the TCR-CD3 Complex. Cell Rep, 14(12), 2833-2845. doi:10.1016/j.celrep.2016.02.081

Pacini, S., et al. (2000). Temporally regulated assembly of a dynamic signaling complex associated with the activated TCR. Eur J Immunol, 30(9), 2620-2631. doi:10.1002/1521-4141(200009)30:9<2620::Aid-immu2620>3.0.Co;2-q

Recio, M. J., et al. (2007). Differential biological role of CD3 chains revealed by human immunodeficiencies. J Immunol, 178(4), 2556-2564. doi:10.4049/jimmunol.178.4.2556

Regueiro, J. R., et al. (1986). Familial defect of CD3 (T3) expression by T cells associated with rare gut epithelial cell autoantibodies. Lancet, 1(8492), 1274-1275. doi:10.1016/s0140-6736(86)91413-3

Reine, J., et al. (2011). CD3gamma-independent pathways in TCR-mediated signaling in mature T and iNKT lymphocytes. Cell Immunol, 271(1), 62-66. doi:10.1016/j.cellimm.2011.06.009

Revy, P., et al. (2019). Somatic genetic rescue in Mendelian haematopoietic diseases. Nat Rev Genet, 20(10), 582-598. doi:10.1038/s41576-019-0139-x

Rieux-Laucat, F., et al. (2006). Inherited and somatic CD3zeta mutations in a patient with T-cell deficiency. N Engl J Med, 354(18), 1913-1921. doi:10.1056/NEJMoa053750

Roberts, J. L., et al. (2007). T-B+NK+ severe combined immunodeficiency caused by complete deficiency of the CD3zeta subunit of the T-cell antigen receptor complex. Blood, 109(8), 3198-3206. doi:10.1182/blood-2006-08-043166

Rodriguez-Gallego, C., et al. (1996). Herpes virus saimiri transformation of T cells in CD3 gamma immunodeficiency: phenotypic and functional characterization. J Immunol Methods, 198(2), 177-186. doi:10.1016/s0022-1759(96)00156-1

San Jose, E., et al. (1998). Assembly of the TCR/CD3 complex: CD3 epsilon/delta and CD3 epsilon/gamma dimers associate indistinctly with both TCR alpha and TCR beta chains. Evidence for a double TCR heterodimer model. Eur J Immunol, 28(1), 12-21. doi:10.1002/(SICI)1521-4141(199801)28:01<12::AID-IMMU12>3.0.CO;2-9

Saveanu, L., et al. (2019). Is there a place and role for endocytic TCR signaling? Immunol Rev, 291(1), 57-74. doi:10.1111/imr.12764

Schamel, W. W., et al. (2019). The TCR is an allosterically regulated macromolecular machinery changing its conformation while working. Immunol Rev, 291(1), 8-25. doi:10.1111/imr.12788

Schatorje, E. J., et al. (2012). Paediatric reference values for the peripheral T cell compartment. Scand J Immunol, 75(4), 436-444. doi:10.1111/j.1365-3083.2012.02671.x

Speckmann, C., et al. (2008). Clinical and immunologic consequences of a somatic reversion in a patient with X-linked severe combined immunodeficiency. Blood, 112(10), 4090-4097. doi:10.1182/blood-2008-04-153361

Sun, J. Y., et al. (1997). Construction of retroviral vectors carrying human CD3 gamma cDNA and reconstitution of CD3 gamma expression and T cell receptor surface expression and function in a CD3 gamma-deficient mutant T cell line. Hum Gene Ther, 8(9), 1041-1048. doi:10.1089/hum.1997.8.9-1041

Sussman, J. J., et al. (1988). Failure to synthesize the T cell CD3-zeta chain: structure and function of a partial T cell receptor complex. Cell, 52(1), 85-95. doi:10.1016/0092-8674(88)90533-8

Takada, H., et al. (2005). Severe combined immunodeficiency caused by a splicing abnormality of the CD-3delta gene. Eur J Pediatr, 164(5), 311-314. doi:10.1007/s00431-005-1639-6

Tiwari, S., et al. (2001). Endoplasmic reticulum (ER)-associated degradation of T cell receptor subunits. Involvement of ER-associated ubiquitin-conjugating enzymes (E2s). J Biol Chem, 276(19), 16193-16200. doi:10.1074/jbc.M007640200

Torres, P. S., et al. (2003). TCR dynamics in human mature T lymphocytes lacking CD3 gamma. J Immunol, 170(12), 5947-5955. doi:10.4049/jimmunol.170.12.5947

Trimble, L. A., et al. (2000). CD3zeta and CD28 down-modulation on CD8 T cells during viral infection. Blood, 96(3), 1021-1029.

Turul, T., et al. (2009). Clinical heterogeneity can hamper the diagnosis of patients with ZAP70 deficiency. Eur J Pediatr, 168(1), 87-93. doi:10.1007/s00431-008-0718-x

Vales-Gomez, M., et al. (2016). Natural killer cell hyporesponsiveness and impaired development in a CD247-deficient patient. J Allergy Clin Immunol, 137(3), 942-945 e944. doi:10.1016/j.jaci.2015.07.051

Wang, H. Y., et al. (2001). Cbl promotes ubiquitination of the T cell receptor zeta through an adaptor function of Zap-70. J Biol Chem, 276(28), 26004-26011. doi:10.1074/jbc.M010738200

Watanabe, N., et al. (2000). The quantity of TCR signal determines positive selection and lineage commitment of T cells. J Immunol, 165(11), 6252-6261. doi:10.4049/jimmunol.165.11.6252

Werner, E. D., et al. (1996). Proteasome-dependent endoplasmic reticulum-associated protein degradation: an unconventional route to a familiar fate. Proc Natl Acad Sci U S A, 93(24), 13797-13801. doi:10.1073/pnas.93.24.13797

Wileman, T., et al. (1990). The gamma and epsilon subunits of the CD3 complex inhibit pre-Golgi degradation of newly synthesized T cell antigen receptors. J Cell Biol, 110(4), 973-986. doi:10.1083/jcb.110.4.973

Yang, M., et al. (1998). Novel aspects of degradation of T cell receptor subunits from the endoplasmic reticulum (ER) in T cells: importance of oligosaccharide processing, ubiquitination, and proteasome-dependent removal from ER membranes. J Exp Med, 187(6), 835-846. doi:10.1084/jem.187.6.835

Zapata, D. A., et al. (2004). Biochemical differences in the alphabeta T cell receptor.CD3 surface complex between CD8+ and CD4+ human mature T lymphocytes. J Biol Chem, 279(23), 24485-24492. doi:10.1074/jbc.M311455200

8. SUPPLEMENTAL INFORMATION

8.1. Normativa y documentos acreditativos para la obtención de Mención de Doctorado Internacional

Normativa (R.D. 99/2011, BOUC 29/04/2015)

Artículo 14. Doctorado Internacional. Requisitos y tramitación (Solo para alumnos matriculados en Programas de Doctorado verificados de acuerdo con el R.D.99/2011)

REQUISITOS: 14.1. El título de Doctor podrá incluir en su anverso la mención «Doctor internacional», siempre que concurran las siguientes circunstancias: **a)** Que el doctorando admitido a un programa de doctorado haya realizado una estancia mínima de tres meses fuera de España en una institución de enseñanza superior o centro de investigación de prestigio, cursando estudios o realizando trabajos de investigación. Dicha estancia podrá ser realizada, como máximo, en dos periodos. La estancia y las actividades han de ser avaladas por el tutor y el director y autorizadas por la Comisión Académica, y se incorporarán al documento de actividades del doctorando. **b)** Que parte de la tesis doctoral, al menos el resumen y las conclusiones, se haya redactado y sea presentada (defendida) en una de las lenguas habituales para la comunicación científica en su campo de conocimiento, distinta a cualquiera de las lenguas oficiales en España. Esta norma no será de aplicación cuando las estancias, informes y expertos procedan de un país de habla hispana. **c)** Que la tesis haya sido informada por un mínimo de dos expertos doctores pertenecientes a alguna institución de educación superior o instituto de investigación no española. **d)** Que al menos un experto perteneciente a alguna institución de educación superior o centro de investigación no española, con el título de doctor, y distinto del responsable de la estancia mencionada en el apartado a), haya formado parte del tribunal evaluador de la tesis.

TRAMITACIÓN: 14.2. El doctorando en el momento de presentar la tesis doctoral tal y como se indica en Artículo 10.6 deberá incorporar la documentación que acredite el cumplimiento de los apartados correspondientes a los requisitos señalados anteriormente. Además, deberá incorporar: **a)** Los dos informes de los expertos señalados en el apartado c) del Artículo anterior acompañados de un breve currículum vitae del investigador que lo emite. (Si pueden estar en el tribunal y pueden ser los evaluadores de la tesis). **b)** Certificación de la estancia fuera de España, con indicación de las fechas inicial y final, emitido por el responsable de la investigación señalada en el apartado a) del Artículo anterior. (No pueden estar en el tribunal) La Comisión Académica del programa, a la vista de la documentación aportada, resolverá si el doctorando puede optar a la Mención Internacional. Si la resolución es positiva, la Comisión Académica remitirá el certificado de la estancia y los informes de los expertos a la Comisión de Doctorado, junto con la propuesta de tribunal y la documentación indicada en el Artículo 10.8. Tras el acto de defensa de la tesis, el Secretario del tribunal certificará el cumplimiento de los apartados b) y d) del Artículo 14.1.

El Presidente de la Comisión de Doctorado, una vez recibida la documentación de la lectura de la tesis, emitirá certificado que se hará llegar al doctorando de la concesión de la mención internacional y en el que se hará constar el cumplimiento de los requisitos indicados en el Artículo 14.1.

8.2. Curriculum vitae

Ana V. Marin, PhD Candidate

ORCID: http://orcid.org/0000-0002-7541-3729

ResearcherID: K-2446-2014

Phone: +34.91.394.1640

anavictoriamarin@ucm.es

Education

Sep 2014 - to date	**PhD Biochemistry, Biology and Biomedicine Candidate.** Complutense University of Madrid (UCM), Spain. Supervisors: Prof. José R. Regueiro (UCM) and Prof. George C. Tsokos (BIDMC-Harvard)
Sep 2011 – Jun 2012	**MSc in Research in Immunology.** UCM, Spain.
Sep 2005 – Jun 2011	**BSc, Biochemistry.** UCM, Spain.

Research Experience

Aug 2020 - to date	**Associated Researcher,** Lymphocyte integration of TCR and complement cues (LITC) (RTI2018-095673-B-I00). Main researchers: José R. Regueiro and Edgar Fernández-Malavé. Dpt. of Immunology, ophthalmology and ORL (IOO), School of Medicine, UCM. Madrid, Spain.
May 2016 – Aug 2020	**Complutense University (UCM)-Harvard Fellow (CT46/15).** Supervisor: José R. Regueiro. Dpt. of IOO, School of Medicine, UCM. Madrid, Spain.
Jan 2013 – Dec 2015	**Associated Researcher,** Biology and physiopathology of the complement system (S2010/BMD-2316). Main researcher: Santiago Rodriguez de Córdoba. Dpt. of IOO, School of Medicine, UCM. Madrid, Spain.
Sep 2011 – Jun 2012	**Master Thesis,** Master of Research in Immunology. "Impact of Ras protein deficiency on the development of functional lineages of Tγδ and iNKT lymphocytes". Supervisor: Dr. Edgar Fernández-Malavé. Dpt. of IOO, School of Medicine, UCM. Madrid, Spain.
Sep 2010 – Jun 2011	**Collaboration Grant.** Supervisor: Dr. Edgar Fernández-Malavé**.** Dpt. of IOO, School of Medicine, UCM. Madrid, Spain.
Sep 2010 – Jun 2011	**Internships.** "Impact of Ras protein deficiency on the development of functional lineages of T lymphocytes". Supervisor: Dr. Edgar Fernández-Malavé. Dpt. of IOO, School of Medicine, UCM. Madrid, Spain.

Teaching Experience

Sep 2017 – Dec 2017	**Co-supervisor of Visiting Researchers** (Janmejay Hingu, The College of New Jersey, USA). Dpt. of IOO, School of Medicine, UCM. Madrid, Spain.
Jun 2015 – Jul 2015	**Co-supervisor of Visiting Researchers** (Luke Pasick, The College of New Jersey, USA). Dpt. of IOO, School of Medicine, UCM. Madrid, Spain.
Sep 2011 – to date	**University Teaching Assistant (**Immunology laboratory practices), Dpt. of IOO, School of Medicine, UCM. Madrid, Spain.

Scientific publications

(See section 8.3)

Books chapters

Marin AV, Recio MJ, Briones AC, Regueiro JR. *Diagnóstico y monitorización inmunológica de las inmunodeficiencias primarias y secundarias*. Ed. Elsevier España, Barcelona, pp 1-11 (2018). ISBN: 978-84-9022-885-2. eISBN: 978-84-9113-341-4.

Research stays

Jun-Sep 2019. Beth Israel Deaconess Medical Center (BIDMC) - Division of Rheumatology; Harvard Medical School Teaching Hospital. Supervisor: George C. Tsokos, MD.

Sep-Nov 2018. Beth Israel Deaconess Medical Center (BIDMC) - Division of Rheumatology; Harvard Medical School Teaching Hospital. Supervisor: George C. Tsokos, MD.

Conference Contributions

Attendance to several national and international meetings with frequent posters and some selected oral communications as first author*:

Jan 2019	*9th Annual Meeting of the Immunology Society of the Community of Madrid (CAM). Madrid, Spain.
Oct 2018	18th Biennial Meeting of the European Society of Immunodeficiencies (ESID). Lisbon, Portugal.
Sep 2018	27th International Complement Workshop. Santa Fe, New Mexico, USA.
Jun 2018	PhDay of School of Medicine, UCM. Madrid, Spain.
Oct 2017	*2nd Meeting of the B cell Network (Net-B). Madrid, Spain.
Jun 2017	PhDay of School of Medicine, UCM. Madrid, Spain.
May 2017	Spanish Congress of Immunology. Zaragoza, Spain.
May 2017	*Jeffrey Modell Foundation Junior Camp 2017. Prague, Czech Republic.
Nov 2016	7th Annual Meeting of the Immunology Society of the CAM. Madrid, Spain.
Sep 2016	17th Biennial Meeting of the ESID. Barcelona, Spain.
Sep 2016	EMBO Conference: Lymphocyte antigen receptor signalling. Siena, Italy.
May 2016	Spanish Congress of Immunology. Alicante, Spain.
Sep 2015	4th European Congress of Immunology. Vienna, Austria.
Jun 2015	15th European Meeting on Complement in Human Disease. Uppsala, Sweden.
Oct 2014	16th Biennial Meeting of the European Society of Immunodeficiencies (ESID). Prague, Czech Republic.
May 2014	*Spanish Congress of Immunology. Badajoz, Spain.
Dec 2013	*4th Annual Meeting of the Immunology Society of the Community of Madrid. Madrid, Spain.
May 2013	*Spanish Congress of Immunology. Salamanca, Spain.
Nov 2012	*7th European Workshop on Immune-Mediated Inflammatory Diseases. Noordwijk, Netherlands.
Oct 2010	9th joint meeting of the International Cytokine for Interferon and Cytokine Research. Florence, Italy.

Skills & Activities

SKILLS	Biochemistry: Western Blotting. Molecular biology: Directed mutagenesis. Cell Biology: Flow cytometry, cell and tissue immunofluorescence, cell culture, magnetic-activated or similar cell sorting, confocal microscopy, T and B cell immortalization, transwell migration assays, *in vitro* T cell activation. Animal handling: mouse, category B. Software: FlowJo, CellQuest Pro, ImageJ, Image Studio, Endnote, GraphPad, Office, Illustrator, Photoshop.
LANGUAGES	Spanish English (C1.2 level)
SCIENTIFIC MEMBERSHIPS	Spanish Society of Immunology (SEI)

8.3. Scientific publications

A. Papers related to PhD project

A.1. Published

1. Katsuyama E, Suarez-Fueyo A, Bradley SJ, Mizui M, **Marin AV**, Mulki L, Krishfield S, Malavasi F, Yoon J, Sui SJH, Kyttaris VC, Tsokos GC. The CD38/NAD/SIRTUIN1/EZH2 Axis Mitigates Cytotoxic CD8 T Cell Function and Identifies Patients with SLE Prone to Infections. **Cell Rep.** 2020 Jan 7;30(1):112-123. e4. doi: 10.1016/j.celrep.2019.12.014. IF 7.85, Q1. Original article

2. **Marin AV**, Jiménez-Reinoso A, Briones AC, Muñoz-Ruiz M, Aydogmus C, Pasick LJ, Couso J, Mazariegos MS, Alvarez-Prado AF, Blázquez-Moreno A, Cipe FE, Haskologlu S, Dogu F, Morín M, Moreno-Pelayo MA, García-Sánchez F, Gil-Herrera J, Fernández-Malavé E, Reyburn HT, Ramiro AR, Ikinciogullari A, Recio MJ, Regueiro JR, Garcillán B. Primary T-cell immunodeficiency with functional revertant somatic mosaicism in CD247. **J Allergy Clin Immunol.** 2017 Jan;139(1):347-349.e8. doi: 10.1016/j.jaci.2016.06.020. Epub 2016 Aug 21. IF 12.48, Q1. Original article

3. Valés-Gómez M, Esteso G, Aydogmus C, Blázquez-Moreno A, **Marin AV**, Briones AC, Garcillán B, García-Cuesta EM, López Cobo S, Haskologlu S, Moraru M, Cipe F, Dobbs K, Dogu F, Parolini S, Notarangelo LD, Vilches C, Recio MJ, Regueiro JR, Ikinciogullari A, Reyburn HT. Natural killer cell hyporesponsiveness and impaired development in a CD247-deficient patient. **J Allergy Clin Immunol**. 2016 Mar;137(3):942-5.e4. doi: 10.1016/j.jaci.2015.07.051. IF 12.48, Q1. Original article

4. Garcillán B, **Marin AV**, Jiménez-Reinoso A, Briones AC, Muñoz-Ruiz M, García- León MJ, Gil J, Allende LM, Martínez-Naves E, Toribio ML, Regueiro JR. γδ T Lymphocytes in the Diagnosis of Human T Cell Receptor Immunodeficiencies. **Front Immunol.** 2015 Jan 29;6:20. doi: 10.3389/fimmu.2015.00020. IF 5.70, Q1. Review article

A.2. Submitted 2020

5. Garcillán B, Mazariegos MS, Jiménez-Reinoso A, **Marin AV**, Muñoz-Ruiz M, Fernández-Malavé E and Regueiro JR. CD3G or CD3D knock-down in mature T lymphocytes similarly cripples the human TCRαβ complex. **Front Cell Dev Biol.** IF 5.20, Q2. Original article

A.3. Under preparation

6. **Marin AV**, Roda-Navarro P and Regueiro JR. TCR dynamics in human CD3δ and CD247 deficiency.

7. Garcillán B, Jiménez-Reinoso A, **Marin AV**, Mazariegos MS, Muñoz-Ruiz M and Regueiro JR. Differential diagnosis of human TCR/CD3 deficiencies.

B. Other papers

B.1. Published

8. **Marin AV**, Cárdenas PP, Jiménez-Reinoso A, Muñoz-Ruiz M, Regueiro JR. Lymphocyte integration of complement cues. **Semin Cell Dev Biol.** 2019 Jan;85:132-142. IF 6.61, Q1. Review article

9. Bravo García-Morato M, Aracil Santos FJ, Briones AC, Blázquez Moreno A, Del Pozo Maté Á, Domínguez-Soto Á, Beato Merino MJ, Del Pino Molina L, Torres Canizales J, **Marin AV**, Vallespín García E, Feito Rodríguez M, Plaza López Sabando D, Jiménez-Reinoso A, Mozo Del Castillo Y, Sanz Santaeufemia FJ, de Lucas-Laguna R, Cárdenas PP, Casamayor Polo L, Coronel Díaz M, Valés-Gómez M, Roldán Santiago E, Ferreira Cerdán A, Nevado Blanco J, Corbí ÁL, Reyburn HT, Regueiro JR, López-Granados E, Rodríguez Pena R. New human combined immunodeficiency caused by interferon regulatory factor 4 (IRF4) deficiency inherited by uniparental isodisomy. **J Allergy Clin Immunol.** 2018 May;141(5):1924-1927.e18. doi: 10.1016/j.jaci.2017.12.995. IF 13.08, Q1. Original article

10. Jiménez-Reinoso A, **Marin AV**, Subias M, López-Lera A, Román-Ortiz E, Payne K, Ma CS, Arbore G, Kolev M, Freeley SJ, Kemper C, Tangye SG, Fernández-Malavé E, Rodríguez de Córdoba S, López-Trascasa M, Regueiro JR. Human plasma C3 is essential for the development of memory B, but not T, lymphocytes. **J Allergy Clin Immunol.** 2018 Mar;141(3):1151-1154.e14. doi: 10.1016/j.jaci.2017.09.037. IF 13.08, Q1. Original article

11. Querol-García J, Fernández FJ, **Marin AV**, Gómez S, Fullà D, Melchor-Tafur C, Franco-Hidalgo V, Albertí S, Juanhuix J, Rodríguez de Córdoba S, Regueiro JR, Vega MC. Crystal Structure of Glyceraldehyde-3-Phosphate Dehydrogenase from the Gram-Positive Bacterial Pathogen A. vaginae, an Immunoevasive Factor that Interacts with the Human C5a Anaphylatoxin. **Front Microbiol**. 2017 Apr 10;8:541. doi: 10.3389/fmicb.2017.00541. IF 4.17, Q1. Original article

12. Jiménez-Reinoso A, **Marin AV**, Regueiro JR. Complement in basic processes of the cell. **Mol Immunol.** 2017 Apr;84:10-16. doi: 10.1016/j.molimm.2016.11.011. IF 3.38, Q2. Review article

B.2. Submitted 2020

13. Molina E, García-Gutiérrez L, Perez-Olivares M, G. de Yebenes V, Quevedo L, Acosta JC, **Marin AV**, Ulgiati D, Merino R, Varela I, Regueiro JR, Moreno de Alboran I, Ramiro A and León J. The receptor of the Epstein-Barr virus (CR2/CD21) is a MYC target gene in Burkitt lymphoma cells. **Haematologica**, 2020. IF 7.12, Q1. Original article

14. **Marin AV**, Jiménez-Reinoso A, Briones-Contreras A, Mazariegos MS, Román-Ortiz E, Regueiro JR. T-cell deficiency in Schimke immuno-osseous dysplasia is not cell-intrinsic. **Front Cell Dev Biol**, 2020. IF 5.20, Q2. Original article

B.3. Under preparation

15. **Marin AV**, Juana-Lopez L, Gaspar ML, de Andrés B, Rodriguez de Cordoba S and Regueiro JR. Study of leucocyte biology in mice models of congenital alternative pathway disorders.